

Think with 3D: Geometric Imagination Grounded Spatial Reasoning from Limited Views

Zhangquan Chen^{1*} Manyuan Zhang^{2†} Xinlei Yu³ Xufang Luo⁴ Mingze Sun¹ Zihao Pan²
 Xiang An⁵ Yan Feng² Peng Pei² Xunliang Cai² Ruqi Huang^{1†}
 1. Tsinghua Shenzhen International Graduate School, Tsinghua University
 2. Meituan 3. National University of Singapore 4. Beihang University 5. LMMs-Lab

Abstract

Though recent advances in vision–language models (VLMs) have achieved remarkable progress across a wide range of multimodal tasks, understanding 3D spatial relationships from limited views remains a significant challenge. Previous reasoning methods typically rely on pure text (e.g., topological cognitive maps) or on 2D visual cues. However, their limited representational capacity hinders performance in specific tasks that require 3D spatial imagination. To address this limitation, we propose 3DThinker, a framework that can effectively exploit the rich geometric information embedded within images while reasoning, like humans do. Our framework is the first to enable 3D mentalizing during reasoning without any 3D prior input, and it does not rely on explicitly labeled 3D data for training. Specifically, our training consists of two stages. First, we perform supervised training to align the 3D latent generated by VLM while reasoning with that of a 3D foundation model (e.g., VGGT). Then, we optimize the entire reasoning trajectory solely based on outcome signals, thereby refining the underlying 3D mentalizing. Extensive experiments across multiple benchmarks show that 3DThinker consistently outperforms strong baselines and offers a new perspective toward unifying 3D representations into multimodal reasoning. Our code is available at <https://github.com/zhangquanchen/3DThinker>.

1. Introduction

Spatial understanding is a critical capability for machines to interact with the real 3D world (e.g., embodied AI, autonomous driving) [62, 70, 74, 86]. These systems typically rely on ego-centric, multi-view observations, typically pro-

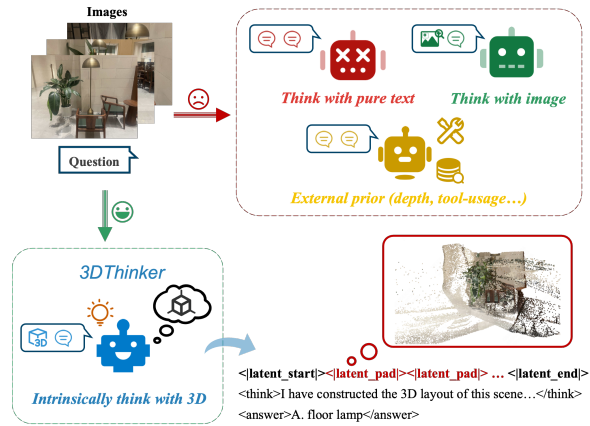


Figure 1. Illustration of our 3DThinker. Existing methods typically perform reasoning based solely on pure text or 2D visual cues, without fully exploiting the rich spatial and geometric information inherent in images. Other methods attempt to enhance the input by introducing auxiliary modalities (e.g., depth maps or coordinates), yet these often depend on additional annotations or external tools. In contrast, our framework enables VLMs to intrinsically form 3D mental representations during reasoning, thereby improving their spatial understanding.

vided by multiple cameras simultaneously capturing limited views of their surroundings. These views are not interchangeable or purely visual; they inherently carry spatial semantics tied to the machine’s frame of reference [24]. Consequently, imagining the full scene and performing reasoning based on a few limited views presents an essential problem for spatial intelligence [80]. Although recent VLMs are pretrained on large-scale image–text corpora, their performance on such spatial reasoning tasks remains notably limited [8, 15, 37, 75]. The core bottleneck lies in their inability to extract 3D geometry embedded within images and their restricted capacity for spatial imagination.

Recent advances have attempted to enhance the spatial reasoning capabilities of VLMs [13, 24, 35, 40, 41, 46, 69]. As illustrated in Fig. 1, existing methods can be broadly divided into two categories. The first category performs

*The work was conducted during the internship of Zhangquan Chen (czq23@mails.tsinghua.edu.cn) at Meituan.

†Corresponding author: ruqihuang@sz.tsinghua.edu.cn, zhang-manyuan@link.cuhk.edu.hk

reasoning with pure text [7, 14, 40, 41, 46] or 2D visual cues [13, 17, 72], whose representational capacity for complex spatial layouts is inherently limited. To mitigate this limitation, methods such as MindCube [83] train models to generate cognitive maps of 3D layouts; however, they rely on bird’s-eye-view (BEV) annotations to construct these maps. Ego3D [24] further employs external models—GroundingDINO [39] for referring expression comprehension (REC) and DepthAnythingv2 [77] for depth estimation, to automatically generate cognitive maps. Yet, constrained by the performance of these models, such methods often fail on low-resolution or uncurated images. The second category incorporates auxiliary modalities as additional inputs (e.g., point clouds, camera parameters) [9, 33]. However, these settings restrict the model’s applicability in real-world scenarios where only monocular images are available. Moreover, several recent methods invoke external encoders or tool-usage to obtain prior information (e.g., encoded 3D tokens [21], depth maps [5, 13, 41]). Importantly, these techniques do not constitute an intrinsic capability of the model and introduce additional inference overhead.

These challenges motivate the need for a new method that: G1) **3D-imaginable**: can directly learn 3D geometry from limited 2D images; G2) **Annotation-free**: does not rely on densely annotated data; and G3) **Intrinsic**: requires no external priors or auxiliary models during inference.

The most relevant mental model, Mirage [80], leverages ground-truth image embeddings for supervised training, facilitating the continuation of a multimodal trajectory without the need for pixel-level image generation. However, the training of [80] is heavily reliant on ground-truth image supervision and remains constrained to the “thinking with image” paradigm, which prevents its effectiveness on (G1) and (G2). Nevertheless, it provides a valuable inspiration, prompting us to *introduce a new novel framework, 3DThinker, which enables thinking with 3D mentaling*. Unlike prior works that depend on external priors or complex training data construction, our method intrinsically integrates 3D representations into the VLMs, enabling unified reasoning and 3D latent generation within the model. For (G1), our framework enables the model to generate geometric representations from images during the reasoning process. Regarding (G2), we directly project the 3D latent to align with a 3D foundation model, thereby circumventing the need for raw 3D data construction. Consequently, our model can inherently “think with 3D” without relying on any prior or auxiliary geometry encoder, corresponding to (G3). Simultaneously, since our method allows for the recovery of 3D representations (e.g., point clouds) from 3D latents via the projector, it *significantly enhances the interpretability of the large reasoning model*.

Specifically, we first construct a batch of Chain-of-Thought (CoT) data that incorporates 3D special tokens.

Our training framework then proceeds in two main stages. In the first stage, we perform supervised learning, where features from the 3D foundation model (e.g., VGGT [60]) are distilled into the native reasoning process of the VLM. To enable the model to think with a 3D mentaling while maintaining textual coherence, we employ both 3D latent alignment loss and the cross-entropy loss. In the second stage, we employ reinforcement learning, optimizing the tokens across the entire sampling trajectory based solely on outcome-driven signals, while preserving the alignment of the 3D latent. That is, we refine 3D mentaling within the trajectory using only outcome as the optimization signal.

Our contributions can be summarized as follows.

- We are the first to introduce the “think with 3D mentaling” framework, which operates without dependence on densely labeled training data (e.g., cognitive maps).
- We propose a two-stage training framework (shown in Fig. 2), progressing from feature alignment to learning intrinsic geometry awareness from outcome-based signals, thus enabling 3D mentaling without any external prior.
- *3DThinker* overcomes the lack of interpretability in latent reasoning. Specifically, *3DThinker* enables the recovery of 3D representations from the latent space via a projector during the reasoning process.
- Extensive experiments across multiple benchmarks demonstrate that *3DThinker* consistently outperforms strong baselines. Furthermore, our results indicate that the effectiveness of *3DThinker* generalizes well across different base VLMs, highlighting its broad applicability.

2. Related Work

2.1. Multimodal Reasoning

Large language models (LLMs) have experienced rapid development, and demonstrated strong performance across a wide range of tasks [11, 16, 36, 71, 82, 85, 88, 96]. Building on these advances, recent works have highlighted that in-context learning, including intermediate rationales, can significantly enhance the performance of LLMs [22, 38, 50, 64, 65, 84, 97]. Current reasoning methods can be categorized into three types: pure-text, visual, and latent reasoning.

Pure-text reasoning: [3, 10, 27, 30, 54, 57] elicit textual step-by-step reasoning inspired by [25]. They typically rely on textual descriptions, which can limit the reasoning capabilities when dealing with visual evidence that cannot be adequately described using pure textual language. **Visual reasoning:** to solve the problem mentioned above, some methods integrate visual evidence directly into the reasoning trajectory, whether in multi-hop or continuous modes. Some intrinsic multi-hop methods [12, 40, 52, 63], first generate detailed visual cues within the model itself (e.g., bounding boxes, coordinates, or masks), and then the

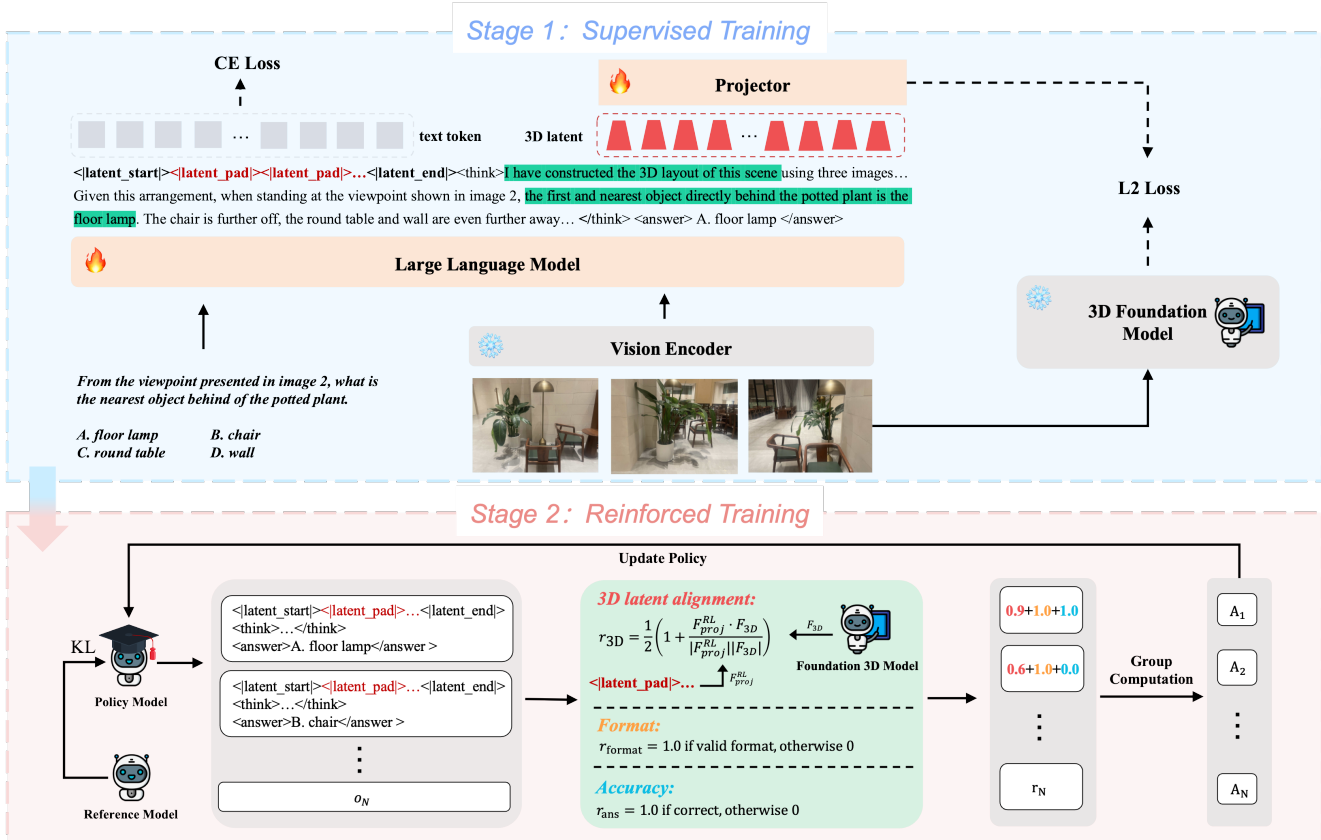


Figure 2. The schematic illustration of our *3DThinker*, a framework that enables thinking with 3D mentaling. (1) Stage 1: *3DThinker* is first trained under supervision using our constructed CoT data (see Sec. 3.1), aligning the generated 3D latents with the feature space of 3D foundation model. This alignment allows the model to leverage suitable 3D spatial mentaling while reasoning. (2) Stage 2: After supervised training, we further optimize the entire trajectory using only outcome signals, while maintaining the alignment of the 3D latents.

further reasoning is conducted based on these cues. Other extrinsic tool-usage methods [45, 55, 68, 95], enhance the “think with image” capability by dynamically invoking external image tools. On the other hand, continuous methods like GRIT [20] and SIFThinker [13] generate continuous visual reasoning to enable iterative corrections during the single-step reasoning process. **Latent reasoning:** some studies have shown that incorporating intermediate hidden representations into LLMs can effectively enhance model capabilities [4, 18, 56, 78]. [26] replaces CoT tokens with continuous latent embeddings, allowing unconstrained reasoning in the latent space to tackle complex tasks. More recently, Mirage [80] and LVR [32] utilize special visual tokens alongside ordinary text during reasoning. They explore visual information within the model by implicitly supervising the generation of image latent, thereby enabling reasoning with 2D visual latent.

While prior works primarily focus on enhancing reasoning ability in textual or 2D spaces, our method takes a different perspective: *we treat latent tokens as a bridge for the model to think with 3D at a mental-level, aligning more closely with human cognition.*

2.2. Spatial Understanding

Spatial understanding encompasses skills such as 3D imagination and spatial cognition, which are essential for perceiving and manipulating spatial relationships in both 2D and 3D environments [6, 19, 43, 44, 59, 73, 81, 87, 89, 90]. Recently, many efforts have been dedicated to evaluating the spatial understanding ability of VLMs [24, 31, 42, 49, 83, 92, 93]. Additionally, several methods have been proposed to enhance spatial understanding. For example, [5, 17, 41, 46, 47] equip LLM with additional multiview, depth or point cloud inputs, essentially serving as input enhancement. Furthermore, 3DRS [28] introduces a teacher model for 3D supervision to achieve explicit spatial representation alignment; however, this method requires input that includes the 3D coordinates corresponding to each pixel. Moreover, VLM-3R [21] employs implicit 3D tokens from a pre-trained model (e.g., CUT3R [61]) to achieve spatial awareness by incorporating prior information, necessitating inference with an extensively 3D foundation model. Recently, methods like MindCube [83] and Ego3D-VLM [24] have facilitated spatial understanding by constructing textual cognitive maps.

Despite these advancements, existing methods often rely on input enhancement or constructed cognitive maps, necessitating complex data collection and annotation. However, *3DThinker* enables 3D mentaling directly from multi views by learning 3D latent distilled from 3D foundation models, thereby facilitating spatial reasoning without relying on densely annotated data.

3. Methodology

Human cognition is inherently rooted in the comprehension of 3D environments. Inspired from the cognitive mechanism of mental imagery, we propose *3DThinker*, a framework that enables VLMs to imagine 3D scenes during reasoning processes. In contrast to existing methods that reason with pure text or 2D visual cues, our framework integrates 3D representations into the interleaved multimodal trajectories. Specifically, *3DThinker* generates compact latent embeddings that serve as 3D tokens, closely emulating the mental 3D scenes that humans intuitively imagine in spatial reasoning. As illustrated in Fig. 2, *3DThinker* first aligns the VLM-generated 3D latent with the 3D foundation model, followed by reinforced training to optimize the trajectory. In this section, we will explain how we achieve this from three aspects: data generation, supervised training (stage 1), and reinforcement training (stage 2).

3.1. Data Generation

Due to the fact that VLMs naturally only generate textual tokens, they require additional supervised training to learn how to produce interleaved reasoning patterns that incorporate 3D information. Therefore, we synthesize specific training corpora based on the raw question-answer data accompanied by multi-view images. Given the image set $\mathcal{I} = \{I_1, I_2, \dots, I_n\}$, a question Q , and the ground truth response R , we employ a high-level model (i.e., GPT-4.1) M to complete the reasoning chain. Specifically, we prompt the model M to generate step-by-step reasoning that contains placeholders (3D special tokens), where these tokens represent imagined 3D scenes in the mind. Denote the response o as:

$$o = M(Q, \mathcal{I}, R). \quad (1)$$

Here, o represents the step-by-step reasoning process with embedded 3D placeholders, whose last layer hidden states are required to be consistent with features extracted from the 3D foundation model during supervised training. By prompting the large-scale reasoning VLM with various inputs, we are able to collect a training dataset $\mathcal{D} = \{(Q^{(i)}, \mathcal{I}^{(i)}, R^{(i)}, o^{(i)})\}$, where each $o^{(i)}$ contains interleaved text and 3D placeholders.

3.2. Supervision for 3D Grounded Reasoning

To teach the model reasoning with 3D, a naive solution is to explicitly align its outputs with 3D representations

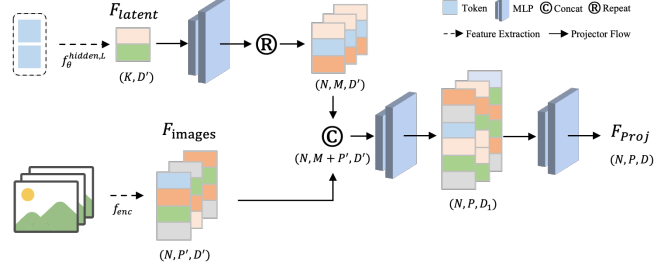


Figure 3. Illustration of our projector, which transforms VLM-generated 3D latent into the feature space of VGGT.

(e.g., point cloud). However, this often depends on labor-intensive data annotation and requires the model to have explicit 3D generation capabilities, which can be quite challenging. Instead, we introduce the 3D foundation model (i.e., VGGT [60]) during training, and distill its features to the 3D special token generated within the VLM reasoning process, thereby facilitating effective *3D-aware reasoning without the need for exhaustive manual labeling*.

Specifically, for each training example $(Q, \mathcal{I}, R, o) \in \mathcal{D}$, the reasoning trajectory o can be decomposed into three sequential components through concatenation operations:

$$o = o_{\text{pre}} \oplus t_{3\text{D}} \oplus o_{\text{post}}, \quad (2)$$

where $t_{3\text{D}} = \{t_1, \dots, t_k\}$ represents the token sequence of human-like 3D mental imagery. The salient vectors $F_{\text{latent}} = \{h_1, \dots, h_k\}$, which operationalize the 3D cognitive tokens $t_{3\text{D}}$, are extracted from the last layer hidden states of VLM $f_{\theta}(\cdot)$ with parameter θ . These salient vectors are recursively generated conditioned on the preceding context:

$$h_i = \begin{cases} f_{\theta}^{\text{hidden},L}(Q, \mathcal{I}, o_{\text{pre}}), & i = 1, \\ f_{\theta}^{\text{hidden},L}(Q, \mathcal{I}, o_{\text{pre}}, t_{1:i-1}), & i \geq 2. \end{cases} \quad (3)$$

Concurrently, we can obtain patch-level visual features $F_{\text{images}} = f_{\text{enc}}(\mathcal{I})$ from the image encoder, and acquire the geometry features $F_{3\text{D}} = f_{\text{vggt}}(\mathcal{I})$ through the last layer of VGGT aggregator. To ensure dimensional consistency between the generated 3D latent features and the predicted geometry features, we employ the projector as illustrated in Fig. 3 to transform F_{latent} into a compatible feature space:

$$F_{\text{proj}} = \text{Projector}(F_{\text{latent}}, F_{\text{images}}). \quad (4)$$

Our objective is to achieve optimal alignment between the projected 3D features derived from the VLM and the corresponding VGGT features. To this end, we formulate the 3D alignment as the Frobenius loss:

$$\mathcal{L}_{3\text{D}} = \|F_{\text{proj}} - F_{3\text{D}}\|_F^2. \quad (5)$$

On the other hand, to ensure textual coherence while introducing 3D tokens, we employ cross-entropy loss to optimize the prediction of surrounding textual tokens. Specifically, the prediction of $i - th$ textual tokens before is $t_{3\text{D}}$

conditioned on both the preceding response tokens and the original input sequence.

$$\mathcal{L}_{\text{text}}^{\text{pre}} = \sum_{i=1}^{|\mathcal{O}_{\text{pre}}|} \ell_{\text{CE}}(o_{\text{pre},i}, f_{\theta}(Q, \mathcal{I}, o_{\text{pre},<i})) \quad (6)$$

In contrast, textual tokens positioned after t_{3D} incorporates k textual 3D special tokens.

$$\mathcal{L}_{\text{text}}^{\text{post}} = \sum_{i=1}^{|\mathcal{O}_{\text{post}}|} \ell_{\text{CE}}(o_{\text{post},i}, f_{\theta}(Q, \mathcal{I}, o_{\text{pre}}, t_{3D}, o_{\text{post},<i})) \quad (7)$$

Finally, the textual loss is formulated as follows:

$$\mathcal{L}_{\text{text}} = \mathcal{L}_{\text{text}}^{\text{pre}} + \mathcal{L}_{\text{text}}^{\text{post}} \quad (8)$$

The overall training objective incorporates both 3D alignment and textual losses, thereby enabling the model to seamlessly incorporate 3D imaging into its textual reasoning process. Here, λ_{3D} and λ_{text} serve as hyperparameters that balances coefficients.

$$\mathcal{L}_{\text{total}} = \lambda_{3D} \mathcal{L}_{3D} + \lambda_{\text{text}} \mathcal{L}_{\text{text}} \quad (9)$$

3.3. Reinforced Spatial Mentaling

At the supervised training stage, our primary objective is to enable the model to perform textual reasoning while simultaneously generating formatted 3D tokens. Additionally, we pre-train the projector to achieve effective alignment of 3D latents. During the reinforced training stage, we expect to use *only outcome signals* to optimize the sampling trajectories and refine the imagined mental 3D representations as well. Specifically, we employ outcome-based group-relative policy optimisation (GRPO) [53], while VGGT features are utilized to further optimize the 3D visual token generated by the model. Notably, the projector remains frozen in this stage. We formalize the RL framework as follows.

For each question-images pair (Q, \mathcal{I}) , the reinforcement learning (RL) framework generates a set of candidate completions $\{o_1, \dots, o_N\}$ from the current policy $\pi_{\theta_{\text{old}}}$, and subsequently updates the policy to π_{θ} by maximizing the following objective:

$$\mathcal{J}(\theta) = \frac{1}{N} \sum_{i=1}^N \frac{1}{|O_i|} \sum_{t=1}^{|\mathcal{O}_i|} \left\{ \min \left[\text{clip}(r_{i,t}, 1 - \epsilon, 1 + \epsilon) \hat{A}_{i,t}, r_{i,t} \hat{A}_{i,t} \right] - \beta \mathbb{D}_{\text{KL}}[\pi_{\theta} \parallel \pi_{\text{ref}}] \right\}, \quad (10)$$

where $r_{i,t} = \frac{\pi_{\theta}(o_{i,t}|q, o_{i,<t})}{\pi_{\theta_{\text{old}}}(o_{i,t}|q, o_{i,<t})}$ denotes the likelihood ratio between the updated and old policies at step t . ϵ, β are hyperparameters, and $\mathbb{D}_{\text{KL}}[\pi_{\theta} \parallel \pi_{\text{ref}}]$ represents the KL divergence [51] between the current policy model and the fixed reference model.

The group-normalized advantage, denoted as $\hat{A}_{i,t}$, is calculated by the task-specific reward $r_{i,t}$.

$$\hat{A}_{i,t} = \frac{r_{i,t} - \text{mean}\{r_{1,t}, \dots, r_{N,t}\}}{\text{std}\{r_{i,t}, \dots, r_{N,t}\} + \delta} \quad (11)$$

Next, we will introduce several specifically designed rewards to achieve reinforced spatial mentaling.

Reward for 3D visual token. After the supervised training, the model has begun to exhibit the ability of 3D mentaling during the thinking process. To further optimize the 3D visual token in the reasoning process, we can extract the last layer hidden state of 3D special token t_{3D} (i.e., `<|latent_start|><|latent_pad|> ... <|latent_end|>`) in each trajectory o and perform optimization. Specifically, the projected features F_{proj}^{RL} are computed based on Eq. 4 at step t , with VGGT features F_{3D} serving as constraints during the RL stage. That is, the cosine similarity between the VGGT features and the projected features is calculated to serve as the reward r_{3D} .

$$r_{3D} = \frac{1}{2} \left(1 + \frac{F_{proj}^{RL} \cdot F_{3D}}{\|F_{proj}^{RL}\| \|F_{3D}\|} \right), \quad (12)$$

Reward for outcome-based optimization. We expect to optimize the entire trajectory using only the outcome-based signals, without relying on explicit annotations of intermediate processes. Thus, we design corresponding rewards for both format (r_{format}) and final answer (r_{ans}). **(1) Format reward:** the model’s output should adhere to the format: `...<|latent_start|><|latent_pad|>... <|latent_end|>...<think>...</think><answer>... </answer>`. A reward of 1.0 is assigned to responses that strictly comply with this format. **(2) Answer reward:** we also provide the 0/1 binary reward by comparing the generated answer with the ground truth option. This outcome-based reward is evenly distributed across each token in the trajectory, including 3D visual tokens.

So, the task reward $r_{i,t}$ is a composite signal comprising the sum of three components: $r_{3D}, r_{\text{format}}$ and r_{ans} .

4. Experiments

Evaluation metric. For multiple-choice questions, we use Accuracy, which is calculated based on exact matches between the model’s predictions and the ground truth. For numerical-answer questions, we use Mean Relative Accuracy (MRA) introduced by [76], a metric that measures the closeness of the model’s predictions to the ground truth values. ”Avg.” denotes the mean value of all subset task.

Training. Models marked with * are trained on our Large-Scale Curated Dataset, whereas those without the mark are trained exclusively on MindCube-only. For further details

Table 1. Accuracy comparison of generalist VLMs and our method (*3DThinker*) on MindCube-Tiny and Ego3D-Bench, with our training conducted on stage 1 (S1) and on both stage 1 and stage 2 (S1 + S2). The best results achieved based on different VLMs are **bolded**. The overall/average results of each model are highlighted in **blue**, with the best results among all models highlighted in **red**.

Method	MindCube-Tiny				Ego3D-Bench								
	Rotation	Among	Around	Overall \uparrow	Ego Dist.	Obj. Dist.	Loc.	Ego Mot.	Obj. Mot.	Travel Time	Ego Rel.	Obj. Rel.	Avg. \uparrow
<i>Closed-source Models</i>													
gpt-4o-2024-11-20	37.0	44.8	56.4	46.1	33.2	26.5	28.1	78.1	56.7	36.0	60.5	66.0	48.1
gpt-4.1	45.5	44.2	47.2	45.1	51.7	36.2	41.8	82.7	62.6	44.3	65.7	70.2	56.9
glm-4.5v	28.0	43.0	33.2	37.8	49.9	39.6	48.4	88.8	73.4	40.4	57.1	81.9	59.9
gemini-2.5-pro	84.0	39.7	56.8	52.2	58.5	50.2	61.4	92.9	75.5	43.5	72.8	78.6	66.7
claude-sonnet-4	49.5	42.2	12.8	36.6	48.9	36.5	51.6	81.9	55.1	33.6	53.9	69.5	53.9
doubao-seed-1.6	87.0	35.8	38.0	46.1	55.2	50.8	60.5	89.0	67.3	49.8	71.4	86.0	66.3
o3-2025-04-16	86.5	42.7	66.0	56.6	71.3	59.3	65.6	93.4	80.1	53.5	77.7	83.1	73.0
<i>Qwen2.5-VL Family [2]</i>													
Qwen2.5-VL-3B	37.4	33.3	30.3	33.2	21.5	29.4	28.8	50.3	41.9	30.9	54.1	56.1	39.1
<i>3DThinker-S1</i> _{Qwen2.5-3B}	44.0	64.8	72.4	62.7	36.1	39.4	32.5	54.8	46.2	30.8	64.0	69.7	46.7
<i>3DThinker-S1+S2</i> _{Qwen2.5-3B}	55.5	81.8	75.2	75.2	41.6	46.0	33.1	54.7	53.3	30.8	70.1	76.9	50.8
Qwen2.5-VL-7B	36.5	32.5	38.4	34.7	32.7	31.5	30.5	45.9	44.0	34.5	43.2	66.5	41.1
<i>3DThinker-S1</i> _{Qwen2.5-7B}	43.5	66.3	76.4	64.4	47.9	44.5	36.5	51.9	51.3	39.1	59.1	73.9	50.5
<i>3DThinker-S1+S2</i> _{Qwen2.5-7B}	55.0	83.0	76.0	76.0	54.0	52.3	36.5	52.7	56.6	38.2	66.0	83.1	54.9
Qwen2.5-VL-32B	39.5	34.5	43.6	37.6	45.4	40.7	49.6	75.6	74.1	40.1	54.0	79.0	57.3
<i>3DThinker-S1</i> _{Qwen2.5-32B}	45.0	66.8	77.2	65.1	52.0	51.9	54.8	80.1	79.4	44.3	62.0	83.1	63.5
<i>3DThinker-S1+S2</i> _{Qwen2.5-32B}	56.5	83.2	77.2	76.7	62.2	61.9	54.5	80.2	86.6	43.7	69.9	86.0	68.1
Qwen2.5-VL-72B	40.0	42.5	44.4	42.5	42.4	38.6	54.8	86.8	68.9	38.5	53.3	80.5	58.0
<i>3DThinker-S1</i> _{Qwen2.5-72B}	42.5	68.0	73.6	64.5	49.9	45.9	57.8	85.6	75.6	43.9	58.0	80.8	62.2
<i>3DThinker-S1+S2</i> _{Qwen2.5-72B}	57.0	83.7	77.6	77.1	61.1	59.9	59.7	93.1	84.9	43.7	69.8	87.8	70.0
<i>InternVL3 Family [98]</i>													
InternVL3-8B	37.0	40.3	63.2	45.1	25.8	28.7	29.8	54.1	54.8	36.1	49.9	65.2	43.1
<i>3DThinker-S1</i> _{InternVL3-8B}	43.0	66.8	79.2	65.2	43.8	44.4	32.9	60.6	61.2	46.9	64.1	72.1	53.3
<i>3DThinker-S1+S2</i> _{InternVL3-8B}	55.0	82.5	79.2	76.5	54.6	56.1	36.0	67.2	69.4	46.7	71.0	81.9	60.4
InternVL3-14B	36.0	48.0	55.6	47.5	46.0	35.6	35.9	63.2	65.9	41.6	55.5	70.1	51.7
<i>3DThinker-S1</i> _{InternVL3-14B}	42.0	68.3	77.2	65.4	56.2	49.1	37.3	70.0	71.8	51.1	68.0	77.7	60.2
<i>3DThinker-S1+S2</i> _{InternVL3-14B}	54.5	84.3	77.6	77.0	63.5	59.9	41.3	78.3	80.2	50.0	75.1	84.0	66.5
InternVL3-38B	32.5	48.5	56.0	47.2	35.4	31.0	39.4	66.6	64.9	38.0	61.0	77.3	51.7
<i>3DThinker-S1</i> _{InternVL3-38B}	39.0	68.0	76.8	64.6	44.8	47.0	43.6	73.1	68.6	48.5	71.2	79.1	59.5
<i>3DThinker-S1+S2</i> _{InternVL3-38B}	53.5	85.2	78.0	77.4	54.7	58.1	49.2	86.9	80.4	49.1	79.6	85.9	68.0
InternVL3-78B	38.5	50.5	57.4	49.9	54.6	48.4	50.3	77.7	70.0	44.8	57.0	76.6	59.9
<i>3DThinker-S1</i> _{InternVL3-78B}	43.5	69.0	77.2	66.1	59.8	53.1	52.2	80.1	72.5	53.9	65.1	78.0	64.3
<i>3DThinker-S1+S2</i> _{InternVL3-78B}	57.0	86.2	78.8	78.9	69.9	61.0	61.0	91.9	88.6	54.8	75.3	83.9	73.3

regarding the training dataset, please refer to the Supp. Mat..

Hyper-parameters. For *3DThinker* trained on MindCube-only, in the stage 1, we set the MLP depth to 6, with the learning rate of $1e-4$, latent size of 12, epoch of 10. In Eqn. 9, the hyper-parameters λ_{3D} , λ_{text} are uniformly set to 0.1 and 1, respectively. In the stage 2, we set the balancing coefficient of all three rewards to 1, with the learning rate of $1e-5$, the rollout number of 8. Additional details are provided in the Supp. Mat..

4.1. Benchmarking Generalist VLMs

In this section, we comprehensively investigate different training stages in *3DThinker* across various generalist VLMs. We conduct experiments on MindCube-Tiny [83] and Ego3D-Bench [24], both of which are designed to evaluate the spatial understanding ability from limited views.

As shown in Tab. 1, *3DThinker*-full achieves consistent improvements over the generalist VLMs across all settings. On MindCube-Tiny, the overall performance gain

ranges from **51.8%** to **108.8%**, while on Ego3D-Bench, the improvement spans **18.1%** to **36.9%**. Taking Qwen2.5-VL-3B as an example, *3DThinker* boosts performance on MindCube-Tiny by **88.9%** (62.7 vs. 33.2) after stage 1, and further improves by **19.9%** (75.2 vs. 62.7) after stage 2. Similarly, on Ego3D-Bench, we observe a **19.3%** improvement (46.7 vs. 39.1) after the stage 1 and an additional **8.8%** gain (50.8 vs. 46.7) following the stage 2. Although the performance is slightly weaker on certain sub-tasks, e.g., Travel Time, this can be attributed to the need for *richer contextual information to align the normalized 3D representations with the real-world*. Remarkably, our model is trained without any Ego3D-specific data, yet it still achieves promising results on Ego3D-Bench, demonstrating strong cross-dataset generalization. *This highlights that our "think with 3D" framework effectively enhances the model's generalization capability across diverse spatial understanding scenarios*. It is also worth noting that our best model, *3DThinker-S1+S2*_{Qwen2.5-72B}, outperforms all other models, both open-source and closed-source, in-

Table 2. The evaluation of various baselines on the VSI-Bench [76], SPBench [35], CV-Bench [58], SPAR-Bench [91], ViewSpatial-Bench [34] and MMSI-Bench [79] datasets. [SI] denotes benchmarks with single image, whereas [MV] refers to multi-view images. The best-performing results under each base model are highlighted.

Method	VSI-Bench [76]	SPBench [35]	CV-Bench [58]	SPAR-Bench [91]	ViewSpatial-Bench [34]	MMSI-Bench [79]	Avg.↑
	[MV]	[SI, MV]	[SI]	[SI, MV]	[SI, MV]	[MV]	
<i>Qwen2.5-VL-3B Based Spatial Models</i>							
Qwen2.5-VL-3B [2]	29.4	38.5	70.6	24.6	35.6	26.5	37.5
Spatial-MLLM-4B [66]	47.3	48.4	73.8	35.1	43.6	31.5	46.6
SpatialLadder-3B [35]	45.7	70.6	73.7	34.4	44.2	29.2	49.6
<i>3DThinker-SI</i> _{Qwen2.5-3B*}	53.2	54.8	74.5	52.3	59.5	37.7	55.3
<i>3DThinker-SI+S2</i> _{Qwen2.5-3B*}	59.1	60.2	78.4	58.2	64.7	41.9	60.4
<i>Qwen2.5-VL-7B Based Spatial Models</i>							
Qwen2.5-VL-7B [2]	35.8	42.9	73.0	30.2	37.9	26.9	41.1
SpaceR-7B [46]	44.5	54.0	75.3	37.1	45.5	28.8	47.5
VILASR-7B [67]	45.4	53.9	77.1	37.8	46.1	30.2	48.4
Video-R1 [23]	33.4	42.8	69.6	31.5	36.1	29.4	40.5
<i>3DThinker-SI</i> _{Qwen2.5-7B*}	57.3	61.5	77.9	56.3	61.7	41.5	59.4
<i>3DThinker-SI+S2</i> _{Qwen2.5-7B*}	63.7	68.3	81.1	63.3	68.6	43.3	64.7

cluding the latest O3 model (78.9 vs. 56.6 on MindCube-Tiny, 73.3 vs. 73.0 on Ego3D-Bench).

4.2. Comparisons with Baselines

We evaluate our method against several state-of-the-art (SOTA) approaches across a diverse set of categories. Additional details are provided in the Supp. Mat..

Different Spatial Models. As shown in Tab. 2, we categorize the methods into two groups based on the types of base VLMs and then evaluate them across different benchmarks. For the Qwen2.5-VL-3B-based spatial models, *3DThinker* surpasses the recent SOTA, SpatialLadder-3B, by **11.5%** (55.3 vs. 49.6) in stage 1. This improvement is further enhanced to **21.8%** (62.7 vs. 49.6) following stage 2. When using the Qwen2.5-VL-7B model, our method achieves even more remarkable results. *3DThinker* outperforms the SOTA VILASR-7B by **22.7%** (59.4 vs. 48.4) in stage 1, and by **33.7%** (64.7 vs. 48.4) in stage 2. On the other hand, in contrast to methods that exhibit task-specific overfitting (e.g., SpatialLadder-3B on SPBench), *3DThinker demonstrates consistent improvement across all tasks, highlighting the robust spatial reasoning capability of our method.* Additionally, unlike models such as Video-R1, which struggle on single-view tasks (e.g., underperforming the base model on CV-Bench), *our method demonstrates strong performance on both single-image and multi-view tasks.* This indicates that our 3D mental reasoning framework significantly enhances performance, even in single-image cases.

Different Architectures and Parameter Scales. Tab. 3 compares our method with Ego3D-VLM on Ego3D-Bench across different model series and parameter scales. Although Ego3D-VLM constructs its cognitive map with the aid of external modules—specifically, a referring expression comprehension model (Grounding-DINO-Base [39]) and a depth estimator (Depth-Anything-V2-Metric-Large [77])—*our method, which does not rely on any extrinsic priors at inference, still achieves superior performance.* In particular, on Qwen2.5-VL-3B, *3DThinker*

Table 3. Performance on Ego3D-Bench (Accuracy Avg.) in comparison between *3DThinker* and Ego3D-VLM, employing a series of VLMs with varying parameters. The best is highlighted.

Method	Qwen2.5-VL				InternVL3			
	3B	7B	32B	72B	8B	14B	38B	78B
Ego3D-VLM [24]	44.4	54.3	65.5	69.5	60.1	66.1	68.0	71.8
<i>3DThinker</i>	50.8	54.9	68.1	70.0	60.4	66.5	68.0	73.3

Table 4. Results with Qwen2.5-VL-3B on MindCube-Tiny in terms of different training strategies. The best is highlighted.

Method	MindCube-Tiny			
	Rotation	Among	Around	Overall ↑
raw-QA SFT	34.5	52.5	66.0	52.3
CoT SFT	36.0	54.3	65.2	53.4
Aug-CGMap-FFR-Out-SFT	49.5	52.5	66.4	55.2
Plain-CGMap-FFR-Out-SFT	47.5	62.3	67.6	60.8
<i>3DThinker-SI</i> _{Qwen2.5-3B}	44.0	64.8	72.4	62.7
GRPO	36.5	49.3	64.8	50.6
CoT SFT + GRPO	36.5	55.2	65.6	54.1
Aug-CGMap-FFR-Out-SFT+RL	53.0	76.8	70.0	70.7
Plain-CGMap-FFR-Out-SFT+RL	48.0	79.2	68.4	70.7
<i>3DThinker-SI+S2</i> _{Qwen2.5-3B}	55.5	81.8	75.2	75.2

yields a notable **14.4%** improvement (50.8 vs. 44.4).

4.3. Training Strategies

To further demonstrate the effectiveness of our training paradigm, we compare *3DThinker* against several representative training strategies as shown in Tab. 4. Among them, Aug-CGMap-FFR-Out and Plain-CGMap-FFR-Out serve as SOTA baselines introduced in [83]. Specifically, Aug-CGMap-FFR-Out performs reasoning with the augmented cognitive map (camera-view information included), whereas Aug-CGMap-FFR-Out relies solely on plain cognitive maps without augmentation.

Under supervised training, our method surpasses raw-QA SFT, CoT SFT, and even the cognitive-map-based SFT proposed in [83] by a margin of **3.1%** (62.7 vs. 60.8). The relatively smaller improvement observed in the rotation sub-category can be attributed to its requirement for dynamic spatial imagination. *Since our "think with 3D"*

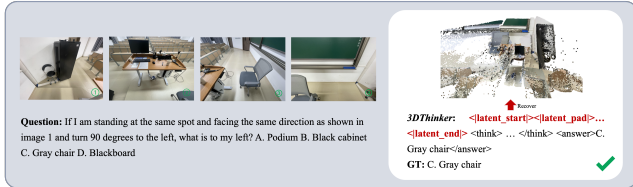
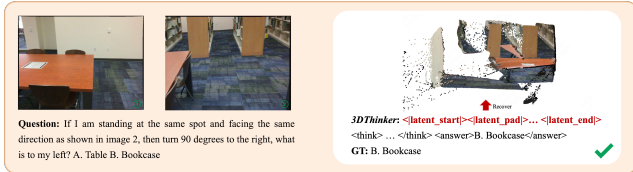


Figure 4. The reasoning process for different cases is presented, along with the visualization of the 3D latent representations.

Table 5. Ablation of different 3D latent size on MindCube-Tiny in terms of $3DThinker-S1_{Qwen2.5-3B}$.

Latent Size	4	8	12	16	32	64
Accuracy	60.2	60.6	62.7	59.9	25.1	15.5

supervised framework primarily targets static spatial understanding, the RL stage further enhances its dynamic capability by optimizing whole reasoning trajectories. That is, through outcome-based RL, $3DThinker$ progressively refines the 3D latents across rollouts, achieving additional gains in both zero-RL and SFT-then-RL settings. Furthermore, $3DThinker$ achieves a **6.4%** improvement over the cognitive-map-based SFT-then-RL baseline (75.2 vs. 70.7), demonstrating its superior capability in integrating spatial reasoning with reinforcement learning.

4.4. Visualization

We visualize the results in Fig. 4. During inference, we extract the last layer hidden states corresponding to the 3D special tokens. These 3D latents are projected into the VGGT feature space via the projector illustrated in Fig. 3. The projected features are subsequently processed by the DPT [48] of VGGT to generate point clouds. As shown in Fig. 4, the reconstructed point clouds roughly depict the underlying scene, where the clearer regions are typically correlated with prompt-relevant objects. This observation indicates that the 3D latents effectively encode the mental scene guided by the prompt intent. After reasoning with 3D mentaling, all two examples yield correct answers. Additional results are provided in the Supp. Mat..

4.5. Ablation Study

Different 3D Latent Size. In Tab. 5, we ablate the effect of different latent sizes on the results. The results indicate that the optimal performance is achieved with the latent size of about 12. *This is because a smaller latent size limits the model’s representational capacity, while a larger latent size can compromise the model’s natural expressive ability, leading to repetitive <|latent_start|> outputs that fail to yield the final answer.*

Table 6. Ablation of different designs including 3D special token position (Token Pos.), projector and rewards in terms of $3DThinker-S1+S2_{Qwen2.5-3B}$ on MindCube-Tiny.

Method	Token Pos.		Projector	Rewards			Full
	Middle	End		w/o r_{format}	w/o r_{ans}	w/o r_{3D}	
Accuracy	42.0	74.3	74.1	74.8	64.2	68.3	75.2

Different Designs. As shown in Tab. 6, we first conduct an ablation study on the placement of the 3D special tokens. Beyond the approach in Sec. 3.3, where the special tokens is positioned at the beginning (before <think>), we also explore placing it between the <think> and </think>, as well as at the end (after </answer>). We observe that placing the 3D tokens in the middle disrupts natural language coherence: *the 3D latent can resemble certain character features, leading to garbled text and premature output termination.* This results in a significant performance drop (75.2 vs. 42.0). In contrast, positioning the 3D tokens at the beginning or end—where it is isolated from natural text—yields significantly better performance.

We also examine two potential projector configurations. The first maps the last layer hidden state of the VLM to the VGGT space (shown in Fig. 3), *allowing the VLM features to be explicitly converted into 3D representations (e.g., point clouds) via the projector.* The alternative compresses VGGT features directly into the VLM space (e.g., via adaptive average pooling), but this approach is unrecoverable to 3D representations. Given the interpretability, visualizability, and better performance (75.2 vs. 74.1) of the first approach, we adopt it as our projector strategy.

Finally, we ablate the three rewards used in stage 2. Among them, the formatting requirement has minimal impact. In contrast, removing 3D alignment leads to a substantial performance drop (75.2 vs. 68.3) due to *the absence of stable constraints on the 3D latent.* The final answer reward is also critical (75.2 vs. 64.2), serving as *the sole ground-truth supervision signal* and guiding optimization of each token across the entire rollout.

5. Conclusion

In this paper, we propose $3DThinker$, a framework for VLM to think with 3D spatial mentaling. Unlike recent methods that rely solely on pure text or 2D visual cues for reasoning, $3DThinker$ leverages geometric information embedded in images during the reasoning process for the first time. Additionally, our method does not rely on dense annotations or other external priors. To enable thinking with 3D spatial mentaling, we introduce a two-stage training scheme. Stage 1 distills geometric features from a pretrained 3D model to warm up. Stage 2 optimizes the entire reasoning trajectory while maintaining 3D visual alignment based on the outcome signal. Experimental results show that our method outperforms previous methods across various benchmarks, establishing a solid foundation for future exploration.

6. Acknowledgments

This work was supported by the National Natural Science Foundation of China under contract No. 62171256.

References

- [1] Xiang An, Yin Xie, Kaicheng Yang, Wenkang Zhang, Xiuwei Zhao, Zheng Cheng, Yirui Wang, Songcen Xu, Changrui Chen, Chunsheng Wu, et al. Llava-onevision-1.5: Fully open framework for democratized multimodal training. *arXiv preprint arXiv:2509.23661*, 2025. 3
- [2] Shuai Bai, Keqin Chen, Xuejing Liu, Jialin Wang, Wenbin Ge, Sibao Song, Kai Dang, Peng Wang, Shijie Wang, Jun Tang, et al. Qwen2. 5-vl technical report. *arXiv preprint arXiv:2502.13923*, 2025. 6, 7
- [3] Sule Bai, Mingxing Li, Yong Liu, Jing Tang, Haoji Zhang, Lei Sun, Xiangxiang Chu, and Yansong Tang. Univg-r1: Reasoning guided universal visual grounding with reinforcement learning. *arXiv preprint arXiv:2505.14231*, 2025. 2
- [4] Eden Biran, Daniela Gottesman, Sohee Yang, Mor Geva, and Amir Globerson. Hopping too late: Exploring the limitations of large language models on multi-hop queries. *arXiv preprint arXiv:2406.12775*, 2024. 3
- [5] Wenxiao Cai, Iaroslav Ponomarenko, Jianhao Yuan, Xiaoqi Li, Wankou Yang, Hao Dong, and Bo Zhao. Spatialbot: Precise spatial understanding with vision language models. *arXiv preprint arXiv:2406.13642*, 2024. 2, 3
- [6] Zhongang Cai, Yubo Wang, Qingping Sun, Ruisi Wang, Chenyang Gu, Wanqi Yin, Zhiqian Lin, Zhitao Yang, Chen Wei, Xuanke Shi, et al. Has gpt-5 achieved spatial intelligence? an empirical study. *arXiv preprint arXiv:2508.13142*, 2025. 3
- [7] Boyuan Chen, Zhuo Xu, Sean Kirmani, Brain Ichter, Dorsa Sadigh, Leonidas Guibas, and Fei Xia. Spatialvlm: Endowing vision-language models with spatial reasoning capabilities. In *Proceedings of the IEEE/CVF Conference on Computer Vision and Pattern Recognition*, pages 14455–14465, 2024. 2
- [8] Boyuan Chen, Zhuo Xu, Sean Kirmani, Brain Ichter, Dorsa Sadigh, Leonidas Guibas, and Fei Xia. Spatialvlm: Endowing vision-language models with spatial reasoning capabilities. In *Proceedings of the IEEE/CVF Conference on Computer Vision and Pattern Recognition*, pages 14455–14465, 2024. 1
- [9] Hanzhi Chen, Boyang Sun, Anran Zhang, Marc Pollefeys, and Stefan Leutenegger. Vidbot: Learning generalizable 3d actions from in-the-wild 2d human videos for zero-shot robotic manipulation. In *Proceedings of the Computer Vision and Pattern Recognition Conference*, pages 27661–27672, 2025. 2
- [10] Liang Chen, Lei Li, Haozhe Zhao, Yifan Song, and Vinci. R1-v: Reinforcing super generalization ability in vision-language models with less than \$3. <https://github.com/Deep-Agent/R1-V>, 2025. Accessed: 2025-02-02. 2
- [11] Zhangquan Chen, Chunjiang Liu, and Haobin Duan. A three-phases-lora finetuned hybrid llm integrated with strong prior module in the education context. In *International Conference on Artificial Neural Networks*, pages 235–250. Springer, 2024. 2
- [12] Zhangquan Chen, Xufang Luo, and Dongsheng Li. Visrl: Intention-driven visual perception via reinforced reasoning. *arXiv preprint arXiv:2503.07523*, 2025. 2
- [13] Zhangquan Chen, Ruihui Zhao, Chuwei Luo, Mingze Sun, Xinlei Yu, Yangyang Kang, and Ruqi Huang. Sifthinker: Spatially-aware image focus for visual reasoning. *arXiv preprint arXiv:2508.06259*, 2025. 1, 2, 3
- [14] An-Chieh Cheng, Hongxu Yin, Yang Fu, Qiushan Guo, Ruihan Yang, Jan Kautz, Xiaolong Wang, and Sifei Liu. Spatialrgpt: Grounded spatial reasoning in vision-language models. *Advances in Neural Information Processing Systems*, 37:135062–135093, 2024. 2
- [15] An-Chieh Cheng, Hongxu Yin, Yang Fu, Qiushan Guo, Ruihan Yang, Jan Kautz, Xiaolong Wang, and Sifei Liu. Spatialrgpt: Grounded spatial reasoning in vision-language models. *Advances in Neural Information Processing Systems*, 37:135062–135093, 2024. 1
- [16] Kexin Chu, Zixu Shen, Dawei Xiang, and Wei Zhang. Safekv: Safe kv-cache sharing in llm serving. In *Machine Learning for Computer Architecture and Systems*, 2025. 2
- [17] Erik Daxberger, Nina Wenzel, David Griffiths, Haiming Gang, Justin Lazarow, Gefen Kohavi, Kai Kang, Marcin Eichner, Yinfei Yang, Afshin Dehghan, et al. Mm-spatial: Exploring 3d spatial understanding in multimodal llms. *arXiv preprint arXiv:2503.13111*, 2025. 2, 3, 1
- [18] Yuntian Deng, Yejin Choi, and Stuart Shieber. From explicit cot to implicit cot: Learning to internalize cot step by step. *arXiv preprint arXiv:2405.14838*, 2024. 3
- [19] Tianqi Ding, Dawei Xiang, Pablo Rivas, and Liang Dong. Neural pruning for 3d scene reconstruction: Efficient nerf acceleration. *arXiv preprint arXiv:2504.00950*, 2025. 3
- [20] Yue Fan, Xuehai He, Diji Yang, Kaizhi Zheng, Ching-Chen Kuo, Yuting Zheng, Sravana Jyothi Narayanaraju, Xinze Guan, and Xin Eric Wang. Grit: Teaching mllms to think with images. *arXiv preprint arXiv:2505.15879*, 2025. 3
- [21] Zhiwen Fan, Jian Zhang, Renjie Li, Junge Zhang, Runjin Chen, Hezhen Hu, Kevin Wang, Huaizhi Qu, Dilin Wang, Zhicheng Yan, et al. Vlm-3r: Vision-language models augmented with instruction-aligned 3d reconstruction. *arXiv preprint arXiv:2505.20279*, 2025. 2, 3
- [22] Guhao Feng, Bohang Zhang, Yuntian Gu, Haotian Ye, Di He, and Liwei Wang. Towards revealing the mystery behind chain of thought: a theoretical perspective. *Advances in Neural Information Processing Systems*, 36:70757–70798, 2023. 2
- [23] Kaituo Feng, Kaixiong Gong, Bohao Li, Zonghao Guo, Yibing Wang, Tianshuo Peng, Junfei Wu, Xiaoying Zhang, Benyou Wang, and Xiangyu Yue. Video-r1: Reinforcing video reasoning in mllms. *arXiv preprint arXiv:2503.21776*, 2025. 7
- [24] Mohsen Gholami, Ahmad Rezaei, Zhou Weimin, Yong Zhang, and Mohammad Akbari. Spatial reasoning with

- vision-language models in ego-centric multi-view scenes. *arXiv preprint arXiv:2509.06266*, 2025. 1, 2, 3, 6, 7
- [25] Daya Guo, Dejian Yang, Haowei Zhang, Junxiao Song, Ruoyu Zhang, Runxin Xu, Qihao Zhu, Shirong Ma, Peiyi Wang, Xiao Bi, et al. Deepseek-r1: Incentivizing reasoning capability in llms via reinforcement learning. *arXiv preprint arXiv:2501.12948*, 2025. 2
- [26] Shibo Hao, Sainbayar Sukhbaatar, DiJia Su, Xian Li, Zhiting Hu, Jason Weston, and Yuandong Tian. Training large language models to reason in a continuous latent space. *arXiv preprint arXiv:2412.06769*, 2024. 3
- [27] Jian Hu, Xibin Wu, Zilin Zhu, Xianyu, Weixun Wang, Dehao Zhang, and Yu Cao. Openrlhf: An easy-to-use, scalable and high-performance rlhf framework. *arXiv preprint arXiv:2405.11143*, 2024. 2
- [28] Xiaohu Huang, Jingjing Wu, Qunyi Xie, and Kai Han. Mllms need 3d-aware representation supervision for scene understanding. *arXiv preprint arXiv:2506.01946*, 2025. 3, 2
- [29] Robert A Jacobs, Michael I Jordan, Steven J Nowlan, and Geoffrey E Hinton. Adaptive mixtures of local experts. *Neural computation*, 3(1):79–87, 1991. 2
- [30] Jiaming Ji, Jiayi Zhou, Hantao Lou, Boyuan Chen, Donghai Hong, Xuyao Wang, Wenqi Chen, Kaile Wang, Rui Pan, Jiahao Li, Mohan Wang, Josef Dai, Tianyi Qiu, Hua Xu, Dong Li, Weipeng Chen, Jun Song, Bo Zheng, and Yaodong Yang. Align anything: Training all-modality models to follow instructions with language feedback. 2024. 2
- [31] Phillip Y Lee, Jihyeon Je, Chanho Park, Mikaela Angelina Uy, Leonidas Guibas, and Minhyuk Sung. Perspective-aware reasoning in vision-language models via mental imagery simulation. *arXiv preprint arXiv:2504.17207*, 2025. 3
- [32] Bangzheng Li, Ximeng Sun, Jiang Liu, Ze Wang, Jialian Wu, Xiaodong Yu, Hao Chen, Emad Barsoum, Muhao Chen, and Zicheng Liu. Latent visual reasoning. *arXiv preprint arXiv:2509.24251*, 2025. 3
- [33] Chengmeng Li, Junjie Wen, Yan Peng, Yaxin Peng, Feifei Feng, and Yichen Zhu. Pointvla: Injecting the 3d world into vision-language-action models. *arXiv preprint arXiv:2503.07511*, 2025. 2
- [34] Dingming Li, Hongxing Li, Zixuan Wang, Yuchen Yan, Hang Zhang, Siqi Chen, Guiyang Hou, Shengpei Jiang, Wenqi Zhang, Yongliang Shen, et al. Viewspatial-bench: Evaluating multi-perspective spatial localization in vision-language models. *arXiv preprint arXiv:2505.21500*, 2025. 7, 1
- [35] Hongxing Li, Dingming Li, Zixuan Wang, Yuchen Yan, Hang Wu, Wenqi Zhang, Yongliang Shen, Weiming Lu, Jun Xiao, and Yueting Zhuang. Spatialladder: Progressive training for spatial reasoning in vision-language models. *arXiv preprint arXiv:2510.08531*, 2025. 1, 7
- [36] Xinjin Li, Yu Ma, Yangchen Huang, Xingqi Wang, Yuzhen Lin, and Chenxi Zhang. Synergized data efficiency and compression (sec) optimization for large language models. In *2024 4th International Conference on Electronic Information Engineering and Computer Science (EIECS)*, pages 586–591, 2024. 2
- [37] Yuan-Hong Liao, Rafid Mahmood, Sanja Fidler, and David Acuna. Reasoning paths with reference objects elicit quantitative spatial reasoning in large vision-language models. *arXiv preprint arXiv:2409.09788*, 2024. 1
- [38] Junhong Lin, Xinyue Zeng, Jie Zhu, Song Wang, Julian Shun, Jun Wu, and Dawei Zhou. Plan and budget: Effective and efficient test-time scaling on large language model reasoning, 2025. 2
- [39] Shilong Liu, Zhaoyang Zeng, Tianhe Ren, Feng Li, Hao Zhang, Jie Yang, Qing Jiang, Chunyuan Li, Jianwei Yang, Hang Su, et al. Grounding dino: Marrying dino with grounded pre-training for open-set object detection. In *European Conference on Computer Vision*, pages 38–55. Springer, 2024. 2, 7
- [40] Yuecheng Liu, Dafeng Chi, Shiguang Wu, Zhanguang Zhang, Yaochen Hu, Lingfeng Zhang, Yingxue Zhang, Shuang Wu, Tongtong Cao, Guowei Huang, et al. Spatialcot: Advancing spatial reasoning through coordinate alignment and chain-of-thought for embodied task planning. *arXiv preprint arXiv:2501.10074*, 2025. 1, 2
- [41] Yang Liu, Ming Ma, Xiaomin Yu, Pengxiang Ding, Han Zhao, Mingyang Sun, Siteng Huang, and Donglin Wang. Ssr: Enhancing depth perception in vision-language models via rationale-guided spatial reasoning. *arXiv preprint arXiv:2505.12448*, 2025. 1, 2, 3
- [42] Wufei Ma, Haoyu Chen, Guofeng Zhang, Yu-Cheng Chou, Celso M de Melo, and Alan Yuille. 3dsrbench: A comprehensive 3d spatial reasoning benchmark. *arXiv preprint arXiv:2412.07825*, 2024. 3
- [43] Chaojun Ni, Xiaofeng Wang, Zheng Zhu, Weijie Wang, Haoyun Li, Guosheng Zhao, Jie Li, Wenkang Qin, Guan Huang, and Wenjun Mei. Wonderturbo: Generating interactive 3d world in 0.72 seconds. *arXiv preprint arXiv:2504.02261*, 2025. 3
- [44] Chaojun Ni, Guosheng Zhao, Xiaofeng Wang, Zheng Zhu, Wenkang Qin, Xinze Chen, Guanghong Jia, Guan Huang, and Wenjun Mei. Recondreamer-rl: Enhancing reinforcement learning via diffusion-based scene reconstruction. *arXiv preprint arXiv:2508.08170*, 2025. 3
- [45] OpenAI. Introducing openai o3 and o4-mini, 2025. <https://openai.com/index/introducing-o3-and-o4-mini/>. 3
- [46] Kun Ouyang, Yuanxin Liu, Haoning Wu, Yi Liu, Hao Zhou, Jie Zhou, Fandong Meng, and Xu Sun. Spacer: Reinforcing mllms in video spatial reasoning. *arXiv preprint arXiv:2504.01805*, 2025. 1, 2, 3, 7
- [47] Zhangyang Qi, Zhixiong Zhang, Ye Fang, Jiaqi Wang, and Hengshuang Zhao. Gpt4scene: Understand 3d scenes from videos with vision-language models. *arXiv preprint arXiv:2501.01428*, 2025. 3
- [48] René Ranftl, Alexey Bochkovskiy, and Vladlen Koltun. Vision transformers for dense prediction. In *Proceedings of the IEEE/CVF international conference on computer vision*, pages 12179–12188, 2021. 8
- [49] Arijit Ray, Jiafei Duan, Reuben Tan, Dina Bashkirova, Rose Hendrix, Kiana Ehsani, Aniruddha Kembhavi, Bryan A Plummer, Ranjay Krishna, Kuo-Hao Zeng, et al. Sat: Spatial aptitude training for multimodal language models. *arXiv preprint arXiv:2412.07755*, 2024. 3

- [50] Ayushman Sarkar, Mohd Yamani Idna Idris, and Zhenyu Yu. Reasoning in computer vision: Taxonomy, models, tasks, and methodologies. *arXiv preprint arXiv:2508.10523*, 2025. 2
- [51] John Schulman. Approximating kl divergence. *John Schulman’s Homepage*, 2020. 5
- [52] Hao Shao, Shengju Qian, Han Xiao, Guanglu Song, Zhuofan Zong, Letian Wang, Yu Liu, and Hongsheng Li. Visual cot: Unleashing chain-of-thought reasoning in multi-modal language models, 2024. 2
- [53] Zhihong Shao, Peiyi Wang, Qihao Zhu, Runxin Xu, Junxiao Song, Xiao Bi, Haowei Zhang, Mingchuan Zhang, YK Li, Y Wu, et al. Deepseekmath: Pushing the limits of mathematical reasoning in open language models. *arXiv preprint arXiv:2402.03300*, 2024. 5
- [54] Haozhan Shen, Zilun Zhang, Qianqian Zhang, Ruochen Xu, and Tiancheng Zhao. Vlm-r1: A stable and generalizable r1-style large vision-language model. <https://github.com/om-ai-lab/VLM-R1>, 2025. Accessed: 2025-02-15. 2
- [55] Zhaochen Su, Linjie Li, Mingyang Song, Yunzhuo Hao, Zhengyuan Yang, Jun Zhang, Guanjie Chen, Jiawei Gu, Juntao Li, Xiaoye Qu, et al. Openthinking: Learning to think with images via visual tool reinforcement learning. *arXiv preprint arXiv:2505.08617*, 2025. 3
- [56] Yu Sun, Yin Li, Ruixiao Sun, Chunhui Liu, Fangming Zhou, Ze Jin, Linjie Wang, Xiang Shen, Zhuolin Hao, and Hongyu Xiong. Audio-enhanced vision-language modeling with latent space broadening for high quality data expansion, 2025. 3
- [57] Omkar Thawakar, Dinura Dissanayake, Ketan More, Ritesh Thawkar, Ahmed Heakl, Noor Ahsan, Yuhao Li, Mohammed Zumri, Jean Lahoud, Rao Muhammad Anwer, Hisham Cholakkal, Ivan Laptev, Mubarak Shah, Fahad Shahbaz Khan, and Salman Khan. Llamav-o1: Rethinking step-by-step visual reasoning in llms, 2025. 2
- [58] Peter Tong, Ellis Brown, Penghao Wu, Sanghyun Woo, Adithya Jairam Vedagiri IYER, Sai Charitha Akula, Shusheng Yang, Jihan Yang, Manoj Middepogu, Ziteng Wang, et al. Cambrian-1: A fully open, vision-centric exploration of multimodal llms. *Advances in Neural Information Processing Systems*, 37:87310–87356, 2024. 7, 1
- [59] Boyuan Wang, Xinpan Meng, Xiaofeng Wang, Zheng Zhu, Angen Ye, Yang Wang, Zhiqin Yang, Chaojun Ni, Guan Huang, and Xingang Wang. Embodiedreamer: Advancing real2sim2real transfer for policy training via embodied world modeling. *arXiv preprint arXiv:2507.05198*, 2025. 3
- [60] Jianyuan Wang, Minghao Chen, Nikita Karaev, Andrea Vedaldi, Christian Rupprecht, and David Novotny. Vggt: Visual geometry grounded transformer. In *Proceedings of the IEEE/CVF Conference on Computer Vision and Pattern Recognition*, 2025. 2, 4
- [61] Qianqian Wang, Yifei Zhang, Aleksander Holynski, Alexei A Efros, and Angjoo Kanazawa. Continuous 3d perception model with persistent state. In *Proceedings of the Computer Vision and Pattern Recognition Conference*, pages 10510–10522, 2025. 3
- [62] Tai Wang, Xiaohan Mao, Chenming Zhu, Runsen Xu, Ruiyuan Lyu, Peisen Li, Xiao Chen, Wenwei Zhang, Kai Chen, Tianfan Xue, et al. Embodiedscan: A holistic multi-modal 3d perception suite towards embodied ai. In *Proceedings of the IEEE/CVF Conference on Computer Vision and Pattern Recognition*, pages 19757–19767, 2024. 1
- [63] XuDong Wang, Shaolun Zhang, Shufan Li, Konstantinos Kallidromitis, Kehan Li, Yusuke Kato, Kazuki Kozuka, and Trevor Darrell. Segllm: Multi-round reasoning segmentation. *arXiv preprint arXiv:2410.18923*, 2024. 2
- [64] Zixuan Wang, Yu Sun, Hongwei Wang, Baoyu Jing, Xiang Shen, Xin Dong, Zhuolin Hao, Hongyu Xiong, and Yang Song. Reasoning-enhanced domain-adaptive pretraining of multimodal large language models for short video content moderation, 2025. 2
- [65] Jason Wei, Xuezhi Wang, Dale Schuurmans, Maarten Bosma, Fei Xia, Ed Chi, Quoc V Le, Denny Zhou, et al. Chain-of-thought prompting elicits reasoning in large language models. *Advances in neural information processing systems*, 35:24824–24837, 2022. 2
- [66] Diankun Wu, Fangfu Liu, Yi-Hsin Hung, and Yueqi Duan. Spatial-mlm: Boosting mllm capabilities in visual-based spatial intelligence. *arXiv preprint arXiv:2505.23747*, 2025. 7
- [67] Junfei Wu, Jian Guan, Kaituo Feng, Qiang Liu, Shu Wu, Liang Wang, Wei Wu, and Tieniu Tan. Reinforcing spatial reasoning in vision-language models with interwoven thinking and visual drawing. *arXiv preprint arXiv:2506.09965*, 2025. 7
- [68] Mingyuan Wu, Jingcheng Yang, Jize Jiang, Meitang Li, Kaizhuo Yan, Hanchao Yu, Minjia Zhang, Chengxiang Zhai, and Klara Nahrstedt. Vtool-r1: Vllms learn to think with images via reinforcement learning on multimodal tool use. *arXiv preprint arXiv:2505.19255*, 2025. 3
- [69] Wenshan Wu, Shaoguang Mao, Yadong Zhang, Yan Xia, Li Dong, Lei Cui, and Furu Wei. Mind’s eye of llms: visualization-of-thought elicits spatial reasoning in large language models. *Advances in Neural Information Processing Systems*, 37:90277–90317, 2025. 1
- [70] Fei Xia, Amir R Zamir, Zhiyang He, Alexander Sax, Jitendra Malik, and Silvio Savarese. Gibson env: Real-world perception for embodied agents. In *Proceedings of the IEEE conference on computer vision and pattern recognition*, pages 9068–9079, 2018. 1
- [71] Dawei Xiang, Wenyan Xu, Kexin Chu, Zixu Shen, Tianqi Ding, and Wei Zhang. Promptsculptor: Multi-agent based text-to-image prompt optimization. *arXiv preprint arXiv:2509.12446*, 2025. 2
- [72] Linhui Xiao, Xiaoshan Yang, Xiangyuan Lan, Yaowei Wang, and Changsheng Xu. Towards visual grounding: A survey. *arXiv preprint arXiv:2412.20206*, 2024. 2
- [73] Wenrui Xu, Dalin Lyu, Weihang Wang, Jie Feng, Chen Gao, and Yong Li. Defining and evaluating visual language models’ basic spatial abilities: A perspective from psychometrics. *arXiv preprint arXiv:2502.11859*, 2025. 3
- [74] Tianyi Yan, Dongming Wu, Wencheng Han, Junpeng Jiang, Xia Zhou, Kun Zhan, Cheng-zhong Xu, and Jianbing Shen.

- Drivingsphere: Building a high-fidelity 4d world for closed-loop simulation. In *Proceedings of the Computer Vision and Pattern Recognition Conference*, pages 27531–27541, 2025. 1
- [75] Tianyi Yan, Junbo Yin, Xianpeng Lang, Ruigang Yang, Cheng-Zhong Xu, and Jianbing Shen. Olidm: Object-aware lidar diffusion models for autonomous driving. In *Proceedings of the AAAI Conference on Artificial Intelligence*, pages 9121–9129, 2025. 1
- [76] Jihan Yang, Shusheng Yang, Anjali W Gupta, Rilyn Han, Li Fei-Fei, and Saining Xie. Thinking in space: How multimodal large language models see, remember, and recall spaces. In *Proceedings of the Computer Vision and Pattern Recognition Conference*, pages 10632–10643, 2025. 5, 7, 1
- [77] Lihe Yang, Bingyi Kang, Zilong Huang, Zhen Zhao, Xiaogang Xu, Jiashi Feng, and Hengshuang Zhao. Depth anything v2. *Advances in Neural Information Processing Systems*, 37:21875–21911, 2024. 2, 7
- [78] Sohee Yang, Elena Gribovskaya, Nora Kassner, Mor Geva, and Sebastian Riedel. Do large language models latently perform multi-hop reasoning? *arXiv preprint arXiv:2402.16837*, 2024. 3
- [79] Sihan Yang, Runsen Xu, Yiman Xie, Sizhe Yang, Mo Li, Jingli Lin, Chenming Zhu, Xiaochen Chen, Haodong Duan, Xiangyu Yue, et al. Mmsi-bench: A benchmark for multi-image spatial intelligence. *arXiv preprint arXiv:2505.23764*, 2025. 7, 1
- [80] Zeyuan Yang, Xueyang Yu, Delin Chen, Maohao Shen, and Chuang Gan. Machine mental imagery: Empower multimodal reasoning with latent visual tokens. *arXiv preprint arXiv:2506.17218*, 2025. 1, 2, 3
- [81] Jiawei Yao and Jusheng Zhang. Depthssc: Depth-spatial alignment and dynamic voxel resolution for monocular 3d semantic scene completion. *arXiv preprint arXiv:2311.17084*, 7:16, 2023. 3
- [82] Jiawei Yao, Chuming Li, and Canran Xiao. Swift sampler: Efficient learning of sampler by 10 parameters. *Advances in Neural Information Processing Systems*, 37:59030–59053, 2024. 2
- [83] Baiqiao Yin, Qineng Wang, Pingyue Zhang, Jianshu Zhang, Kangrui Wang, Zihan Wang, Jieyu Zhang, Keshigeyan Chandrasegaran, Han Liu, Ranjay Krishna, et al. Spatial mental modeling from limited views. *arXiv preprint arXiv:2506.21458*, 2025. 2, 3, 6, 7, 1
- [84] Zhenyu Yu, Mohd Yamani Idna Idris, Hua Wang, Pei Wang, Junyi Chen, and Kun Wang. From physics to foundation models: A review of ai-driven quantitative remote sensing inversion. *arXiv preprint arXiv:2507.09081*, 2025. 2
- [85] Zhenyu Yu, Mohd Yamani Idna Idris, Pei Wang, Yuelong Xia, and Yong Xiang. Forgetme: Benchmarking the selective forgetting capabilities of generative models. *Engineering Applications of Artificial Intelligence*, 161:112087, 2025. 2
- [86] Shuang Zeng, Xinyuan Chang, Mengwei Xie, Xinran Liu, Yifan Bai, Zheng Pan, Mu Xu, and Xing Wei. Futuresight-drive: Thinking visually with spatio-temporal cot for autonomous driving. *arXiv preprint arXiv:2505.17685*, 2025. 1
- [87] Shuang Zeng, Dekang Qi, Xinyuan Chang, Feng Xiong, Shichao Xie, Xiaolong Wu, Shiyi Liang, Mu Xu, and Xing Wei. Janusvln: Decoupling semantics and spatiality with dual implicit memory for vision-language navigation. *arXiv preprint arXiv:2509.22548*, 2025. 3
- [88] Yiming Zeng, Wanhao Yu, Zexin Li, Tao Ren, Yu Ma, Jinghan Cao, Xiyan Chen, and Tingting Yu. Bridging the editing gap in llms: Fineedit for precise and targeted text modifications, 2025. 2
- [89] Jirong Zha, Yuxuan Fan, Xiao Yang, Chen Gao, and Xinlei Chen. How to enable llm with 3d capacity? a survey of spatial reasoning in llm. *arXiv preprint arXiv:2504.05786*, 2025. 3
- [90] J. Zhang, W. Zhang, C. Tan, X. Li, and Q. Sun. Yolo-ppa based efficient traffic sign detection for cruise control in autonomous driving. *arXiv preprint arXiv:2409.03320*, 2024. 3
- [91] Jiahui Zhang, Yurui Chen, Yanpeng Zhou, Yueming Xu, Ze Huang, Jilin Mei, Junhui Chen, Yu-Jie Yuan, Xinyue Cai, Guowei Huang, et al. From flatland to space: Teaching vision-language models to perceive and reason in 3d. *arXiv preprint arXiv:2503.22976*, 2025. 7, 1
- [92] Wenyu Zhang, Wei En Ng, Lixin Ma, Yuwen Wang, Junqi Zhao, Allison Koenecke, Boyang Li, and Lu Wang. Sphere: Unveiling spatial blind spots in vision-language models through hierarchical evaluation. *arXiv preprint arXiv:2412.12693*, 2024. 3
- [93] Weichen Zhang, Zile Zhou, Zhiheng Zheng, Chen Gao, Jinqiang Cui, Yong Li, Xinlei Chen, and Xiao-Ping Zhang. Open3dvqa: A benchmark for comprehensive spatial reasoning with multimodal large language model in open space. *arXiv preprint arXiv:2503.11094*, 2025. 3
- [94] Chujie Zheng, Shixuan Liu, Mingze Li, Xiong-Hui Chen, Bowen Yu, Chang Gao, Kai Dang, Yuqiong Liu, Rui Men, An Yang, et al. Group sequence policy optimization. *arXiv preprint arXiv:2507.18071*, 2025. 2
- [95] Ziwei Zheng, Michael Yang, Jack Hong, Chenxiao Zhao, Guohai Xu, Le Yang, Chao Shen, and Xing Yu. Deep-eyes: Incentivizing “thinking with images” via reinforcement learning. *arXiv preprint arXiv:2505.14362*, 2025. 3
- [96] Pengfei Zhou, Weiqing Min, Chaoran Fu, Ying Jin, Mingyu Huang, Xiangyang Li, Shuhuan Mei, and Shuqiang Jiang. Foodsky: A food-oriented large language model that can pass the chef and dietetic examinations. *Patterns*, 6(5), 2025. 2
- [97] Xiaoling Zhou, Wei Ye, Zhemg Lee, Lei Zou, and Shikun Zhang. Valuing training data via causal inference for in-context learning. *IEEE Transactions on Knowledge and Data Engineering*, 2025. 2
- [98] Jinguo Zhu, Weiyun Wang, Zhe Chen, Zhaoyang Liu, Shenglong Ye, Lixin Gu, Hao Tian, Yuchen Duan, Weijie Su, Jie Shao, et al. Internvl3: Exploring advanced training and test-time recipes for open-source multimodal models. *arXiv preprint arXiv:2504.10479*, 2025. 6

Think with 3D: Geometric Imagination Grounded Spatial Reasoning from Limited Views

Supplementary Material

In this supplementary material, we provide more technical details and experimental results, including 1) Detailed descriptions of training dataset and benchmarks in Sec. 7; 2) Additional results including benchmarking Qwen3-VL and LLaVA-OneVision-1.5, additional baselines, general image understanding, prompt-relevant region, as well as ablation studies on projection methods and 3D loss in Sec. 8; 3) Training curve for two stages of *3DThinker* in Sec. 9; 4) Details of the dataset generation process in Sec. 10; 5) Explanation of the claim in Sec. 11; 6) Cost in Sec. 12; and 7) More “think with 3D” visualization including representative and failure cases in Sec. 13.

7. Dataset

7.1. Training Dataset

MindCube-Only Training: Following [83], we utilize a subset of 10,000 question-images-answer pairs for the training phases in Tab.1 of the main text. That is, in stage 1, we use the 10,000 samples to construct the CoT data for supervised training. In stage 2, we utilize only the question-image-answer pairs of these 10,000 samples for reinforced training. *Notably, no annotated cognitive maps are used in any stage of our training.*

Large-Scale Curated Dataset Training: We further select data from MM-Spatial [17], SPAR [91], MindCube [83], and SpatialLadder [35] to construct a larger-scale dataset. We utilized Gemini 2.5 Pro to evaluate the data quality and balanced the distribution between single-image and multi-image categories, ultimately retaining 237K samples. The methodology for constructing CoT data from standard QA pairs is detailed in Sec. 3.1 in the main text and Sec. 10. Similarly, we employed the complete CoT dataset in stage 1, whereas stage 2 solely utilized the question-image-answer pairs. For the training process, stage 1 was trained on the entire dataset for one epoch, while stage 2 was trained on a sampled subset of 57K instances.

7.2. Benchmarks

MindCube-Tiny [83] contains 1,050 data, serves as the benchmark for evaluation of spatial understanding from limited views. The dataset includes three types of camera movements: Rotation (the camera remains stationary while rotating to observe the surroundings), Around (the camera moves in a circular path around the evaluated objects), and Among (the camera moves in a circular path among the evaluated objects).

Ego3D-Bench [24] is a comprehensive benchmark consisting of over 8,600 question-answer pairs, specifically designed to evaluate the spatial reasoning capabilities of model in ego-centric, multi-view outdoor environments. The dataset encompasses five tasks—Absolute Distance Measurement (Dist.), Relative Distance Measurement (Rel.), Localization (Loc.), Motion Reasoning (Mot.), and Travel Time (Time), each formulated in both ego-centric (Ego) and object-centric (Obj.) settings.

VSI-Bench [76] consists of over 5,000 question-answer pairs derived from 288 real-world videos. These videos encompass a wide variety of environments—including residential areas, professional settings (e.g., offices and laboratories), and industrial sites (e.g., factories), and span multiple geographic regions.

SPBench [35] comprises two different tasks: SPBench-SI and SPBench-MV, corresponding to the single-image and multi-view types, respectively. SPBench-SI includes four categories: absolute distance, object size, relative distance, and relative direction, containing a total of 1,009 samples. SPBench-MV extends the evaluation by incorporating object counting tasks, comprising 319 samples.

CV-Bench [58] contains 2,638 manually inspected examples, each formulated as a natural-language question to assess the fundamental 2D and 3D understanding capabilities of VLMs. The 2D understanding tasks focus on spatial relationships and object counting, while the 3D understanding tasks involve depth ordering and relative distance.

SPAR-Bench [91] covers 20 diverse spatial tasks—including depth estimation, distance measurement, spatial relations, etc. The benchmark spans single-view, multi-view, and video settings, comprising a total of 7,207 manually verified question-answer pairs.

ViewSpatial-Bench [34] focuses on reasoning from alternative spatial frames of reference, requiring models to adopt another entity’s viewpoint. It consists of over 5,700 question-answer pairs derived from more than 1,000 3D scenes. This benchmark evaluates the spatial localization capabilities, specifically assessing both egocentric (camera-centered) and allocentric (human-centered) viewpoints across five distinct task types.

MMSI-Bench [79] comprises 1,000 multiple-choice questions from over 120,000 images. The benchmark focuses on positional relationships (six pairwise combinations of camera, object, and region), attributes (measurement and appearance), and motion (camera and object).

8. Additional Results

8.1. Benchmarking Qwen3-VL and LLaVA-OneVision-1.5

We further conducted experiments on the Qwen3-VL and LLaVA-OneVision-1.5. Note that Qwen3-VL adopts `<think>` as a predefined special token, thus we have modified to `<thinking>` to avoid potential conflicts. On the other hand, we modify the stage 2 from token-level GRPO [25] to sequence-level GSPO [94] for all Mixture-of-Experts(MoE)-based [29] models to maintain stable training.

Qwen3-VL: Tab. 7 shows that our method consistently boosts the spatial understanding capability of Qwen3-VL. On the MindCube-Tiny [83] dataset, *3DThinker* achieves a maximum improvement of **191.5%** (75.8 vs. 25.0), elevating the VLM from random guessing to highly accurate understanding on spatial reasoning tasks. On the Ego3D-Bench [24] dataset, *3DThinker* yields up to a **29.9%** improvement (56.1 vs. 43.2), demonstrating strong generalization ability. Moreover, we validated our method on Qwen3-VL-30B-A3B sparse model as well, confirming the effectiveness of our method across both dense and sparse architectures.

LLaVA-OneVision-1.5: As shown in Tab. 8, we further extended our training to another foundation model. Specifically, on LLaVA-OneVision-1.5, *3DThinker* consistently yielded significant performance gains. Notably, it achieved a **68.07%** (63.7 vs. 37.9) improvement on MindCube-Tiny and a **7.5%** (48.7 vs. 45.3) increase on Ego3D-Bench.

8.2. Additional Baselines

As shown in Tab. 9, *3DThinker* consistently outperforms previous methods, surpassing the SOTA by **8.79%** (65.6 vs. 60.3). This further highlights the effectiveness of incorporating 3D mentaling for spatial reasoning.

8.3. General Image Understanding

As shown in Tab. 10, our method largely maintains, and on some benchmarks even substantially improves. For example, on POPE *3DThinker* outperforms the base model by **2.91%** (88.4 vs. 85.9). On MME, which predominantly consists of 2D image understanding tasks (e.g., OCR, numerical reasoning), our results are still comparable to the base model. These results suggest that *3DThinker* effectively transfers the base model’s 2D image understanding abilities and *exhibits strong robustness*.

8.4. Prompt-Relevant Region

As shown in Fig. 5, we provide a quantitative result to substantiate the claim of “prompt-relevant”. Specifically, we compute the point cloud density within the red 3D bounding

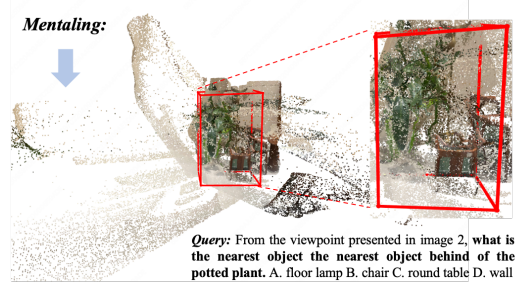


Figure 5. Density calculation for the Mentaled point cloud.

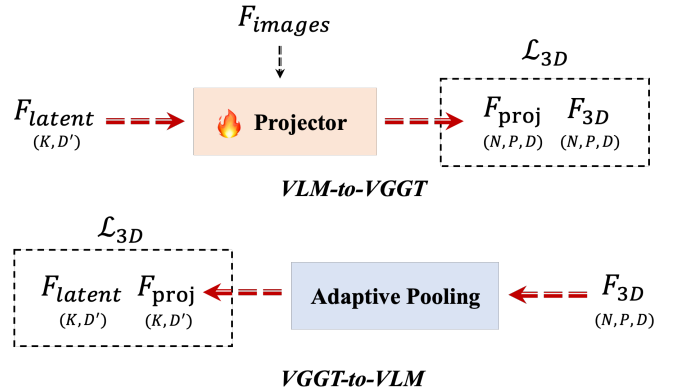


Figure 6. Illustration of two methods for projection. Above: project the latents generated by VLM into the feature space of the 3D foundation model; Below: project the features of the 3D foundation model into the feature space of the VLM.

box and compare it with the overall point cloud density. The resulting densities are **196494.67** vs. 1332.54 points/unit³.

8.5. Ablation on Projection Methods

As illustrated in Fig. 6, we present a more detailed comparison of the two feature alignment strategies. The above method requires training the projector, whereas the below one can be implemented directly via pooling [28] without any training. As discussed in Sec. 4.5, the two methods achieve comparable performance (74.1 vs. **75.2**). However, the above method not only maintains slightly better performance, but also *enables the recovery of 3D representations from the VLM latent space*. Therefore, we adopt the VLM-to-VGGT projection in our framework.

8.6. Ablation on 3D Loss

To evaluate the impact of \mathcal{L}_{3D} on our framework, we further conduct the ablation where the 3D foundation model was removed, and only the cross-entropy loss ($\mathcal{L}_{\text{text}}$) was applied to tokens other than the 3D special token. As shown in Tab. 11, using Qwen2.5-VL-3B as an example, the performance drops from 62.7 (full) to 54.1 without \mathcal{L}_{3D} , though

Table 7. Accuracy comparison between LATEST Qwen3-VL (under varying parameter scales and architectures) and 3DThinker on different benchmarks, with our training conducted on stage 1 (S1) and on both stage 1 and stage 2 (S1 + S2). The best results achieved based on different VLMs are **bolded**. The overall/average results of each model are highlighted in **blue**.

Method	MindCube-Tiny [83]				Ego3D-Bench [24]								
	Rotation	Among	Around	Overall ↑	Ego Dist.	Obj. Dist.	Loc.	Ego Mot.	Obj. Mot.	Travel Time	Ego Rel.	Obj. Rel.	Avg. ↑
Qwen3-VL-2B	29.0	32.2	46.8	35.0	24.7	23.9	30.4	58.7	56.4	32.8	57.4	61.1	43.2
3DThinker-S1 _{Qwen3-2B}	40.5	67.5	77.2	64.7	45.9	41.6	36.0	60.6	59.2	37.2	62.0	72.1	51.8
3DThinker-S1+S2 _{Qwen3-2B}	53.0	83.2	78.4	76.2	53.1	51.3	36.4	61.4	62.8	38.2	65.3	80.5	56.1
Qwen3-VL-4B	34.0	18.7	37.2	26.0	41.3	40.9	27.9	56.9	56.6	37.8	60.1	68.2	48.7
3DThinker-S1 _{Qwen3-4B}	43.0	65.3	76.0	63.6	54.0	49.9	35.1	59.3	60.8	40.8	64.9	76.1	55.1
3DThinker-S1+S2 _{Qwen3-4B}	55.0	81.7	78.4	75.8	62.3	56.5	35.5	61.4	64.1	40.4	68.3	84.0	59.1
Qwen3-VL-8B	31.5	31.0	41.2	33.5	38.9	32.6	31.6	45.3	56.8	40.8	62.4	69.3	47.2
3DThinker-S1 _{Qwen3-8B}	42.0	67.8	76.8	65.0	52.1	45.9	37.1	51.5	61.8	43.2	67.8	78.2	54.7
3DThinker-S1+S2 _{Qwen3-8B}	56.5	82.5	78.8	76.7	63.0	56.8	38.1	55.5	66.2	43.2	71.1	86.1	60.0
Qwen3-VL-32B	29.5	33.5	38.0	33.8	51.5	40.7	40.9	76.4	58.2	40.4	61.5	81.4	56.4
3DThinker-S1 _{Qwen3-32B}	41.0	69.5	77.6	66.1	60.4	51.0	48.3	78.6	67.9	43.2	68.1	87.3	63.1
3DThinker-S1+S2 _{Qwen3-32B}	55.0	84.2	79.6	77.5	69.3	62.2	48.7	85.1	73.5	43.0	73.1	90.3	68.2
Qwen3-VL-30B-A3B	37.0	43.9	45.6	42.9	49.1	45.8	28.4	64.5	60.0	34.7	63.3	73.3	52.4
3DThinker-S1 _{Qwen3-30B-A3B}	46.5	72.8	82.0	70.0	60.1	54.4	38.3	72.2	70.3	38.0	71.0	80.1	60.6
3DThinker-S1+S2 _{Qwen3-30B-A3B}	60.0	86.7	83.2	80.8	69.4	65.1	39.1	79.3	75.1	37.6	76.3	88.0	66.2

Table 8. Accuracy comparison of generalist VLMs and our method (3DThinker) on MindCube-Tiny and Ego3D-Bench, with our training conducted on stage 1 (S1) and on both stage 1 and stage 2 (S1 + S2). The best results achieved based on different VLMs are **bolded**. The overall/average results of each model are highlighted in **blue**, with the best results among all models highlighted in **red**.

Method	MindCube-Tiny				Ego3D-Bench								
	Rotation	Among	Around	Overall ↑	Ego Dist.	Obj. Dist.	Loc.	Ego Mot.	Obj. Mot.	Travel Time	Ego Rel.	Obj. Rel.	Avg. ↑
	<i>LLaVA-OneVision-1.5 Family [1]</i>												
LLaVA-OneVision-1.5-4B	33.5	38.0	49.2	39.8	39.7	37.1	29.2	51.4	51.8	34.1	52.4	73.5	46.2
3DThinker-S1 _{LLaVA-O-1.5-4B}	41.5	59.8	66.0	57.8	40.0	39.1	33.1	51.1	52.6	30.9	58.6	73.8	47.4
3DThinker-S1+S2 _{LLaVA-O-1.5-4B}	48.0	67.5	65.2	63.2	40.2	39.9	34.2	51.9	52.3	30.8	61.8	73.8	48.1
LLaVA-OneVision-1.5-8B	34.5	34.7	48.4	37.9	30.3	36.6	34.3	44.9	51.9	36.9	53.4	74.4	45.3
3DThinker-S1 _{LLaVA-O-1.5-8B}	43.0	57.8	64.8	56.7	35.1	39.0	36.1	44.9	53.2	31.9	61.0	73.8	46.9
3DThinker-S1+S2 _{LLaVA-O-1.5-8B}	49.0	68.2	64.8	63.7	36.5	41.5	37.0	46.2	53.3	32.8	64.9	77.2	48.7

Table 9. Performance comparison of all baselines on 3DSRBench.

SpatialReasoner	SpatialReasoner-R1	SpatialThinker	3DThinker *
60.3	55.7	56.4	65.6

Table 10. Results on general VLM benchmarks.

Method	MME ^P	MME ^C	POPE	SEED-I
Qwen2.5-VL-7B	1670	623	85.9	77.0
3DThinker *	1677	610	88.4	78.9

Table 11. Ablation study on 3D alignment loss on MindCube-Tiny in terms of Qwen2.5-VL-3B.

Method	MindCube-Tiny			
	Rotation	Among	Around	Overall ↑
w/o \mathcal{L}_{3D}	35.0	55.1	66.8	54.1
Full	44.0	64.8	72.4	62.7

it remains slightly higher than the CoT SFT (53.4). These results highlight two key insights: (1) *incorporating the 3D foundation model helps the VLM utilize the special token to encode geometric information*, thereby enhancing the spatial reasoning capability; and (2) *even without the 3D foundation model, introducing special tokens increases the representational flexibility of the model*, leading to moderate

improvements on certain metrics.

9. Training Curve

As shown in Fig. 7, we visualize the training curves of our two-stage process in terms of training on MindCube-only. The loss in stage 1 (**green**) converges after approximately 20k steps, reaching around 0.15. The reward in stage 2 (**blue**) converges much faster, stabilizing after roughly 500 steps with a reward value of about 2.7. In the bottom-right panel, we further plot the curves of the format reward (r_{format}) and the answer reward (r_{ans}). Both exhibit a brief decline during the early phase of training, followed by a steady upward trend. *This initial drop can be attributed to the model’s exploration behavior at the beginning of reinforcement learning*, during which it searches the solution space and may temporarily follow suboptimal trajectories before discovering more optimal ones that lead to rapid performance improvement.

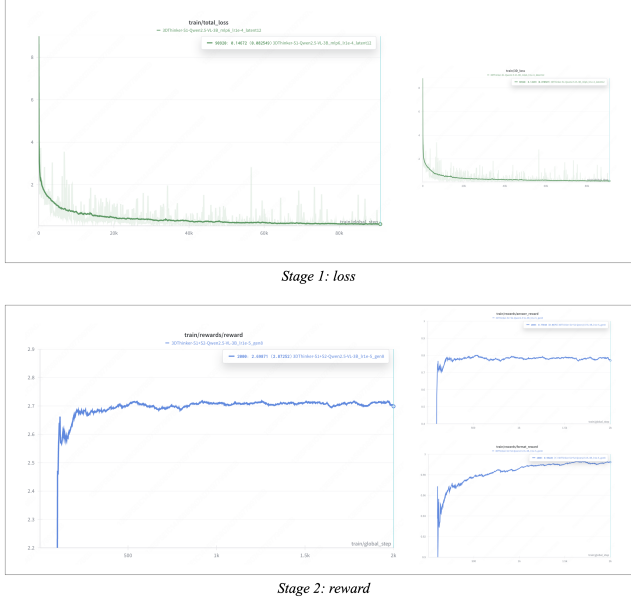


Figure 7. Visualization of our training curves in terms of Qwen2.5-VL-3B on stage 1 (green curves) and stage 2 (blue curves). Top-left: total loss of stage 1; Top-right: 3D loss of stage 1; Bottom-left: total reward of stage 2; Bottom-right: answer reward and format reward of stage 2.

The Question, Images, and Answer are presented as follows. Please help me start with the mental 3D scene special token `<output_3D>` and complete the reasoning chain.

Question: {question},
 Answer: {answer}.

Figure 8. Prompt for the CoT generation, with the input of question and GT answer.

10. Details for Dataset Generation

For the training dataset, which consists of image set from different views I , question Q and GT response R , we employed GPT-4.1 (M) to complete the CoT reasoning process o . Fig. 8 and Fig. 9 illustrate the prompts we designed for generating CoT data. Additionally, we assess the quality of the generated CoT, ensuring that o contains `<output_3D>` at the beginning, followed by the text in adherence to the format `<think>...</think> <answer>...</answer>`. The CoT data o that do not conform to this specification will be re-generated by M . If the data fails to meet the required format after more than $N = 10$ attempts, it will be discarded.

You are an advanced AI reasoning assistant with expertise in 3D spatial understanding. Your task is to complete the intermediate reasoning process using the provided Question, Images, and Answer. To assist your reasoning, you should mentally construct a 3D layout of the scene.

Wrap your reasoning process with `<think></think>` tags and your final result with `<answer></answer>` tags. The mental 3D scene you imagine will be represented by the special token `<output_3D>`, which should be presented at the beginning of your response. Only one `<output_3D>` is allowed, and `</output_3D>` should not be included.

For example:

```
<output_3D>
<think> I have imagined a 3D scene shown above based on the given
images, where there is a white water cup placed on a table. The room
has distinct features on each side, including walls, windows, a fridge,
and possibly furniture like cabinets and chairs. The cameras capturing
the images are positioned at the front, left, back, and right of the cup,
providing different perspectives of the surroundings. From the perspective
of image 1 provided, we notice that there is a window with daylight
coming through, and a fridge is visible next to it. This orientation suggests
that the specific viewpoint from image 1 is facing these objects: the
window and the fridge. In my mind, I imagine adjusting the position of
the 3D scene to align it with the direction shown in image 1. Now, I need
to think about what might be behind the viewpoint based on this setup. I
imagine myself in the 3D scene, walking to the opposite side, that is,
rotating the view horizontally 180 degrees. I saw the Window and fridge,
which is what image 2 shows. So, the answer is B. Window and fridge
</think>
<answer>B. Window and fridge</answer>
```

Figure 9. System prompt for the CoT generation .

11. Explanation of the Claim

Annotation-free: In fact, unlike previous purely textual CoT methods, our method requires 3D mentaling during the reasoning process. Thus, “annotation-free” refers specifically to the absence of *manual geometric annotations for 3D mentaling* (e.g., ground-truth point clouds). In our framework, GPT-4.1 is only used to generate 3D placeholders, while the actual 3D geometric features associated with these placeholders are provided by VGGT aggregator.

VGGT Dependence: In the supervised training stage, we aim to elicit “think with 3D” behaviour without relying on manual geometric annotations, which leads us to make use of features extracted by VGGT. In contrast, learning to generate 3D geometry entirely from scratch would necessitate explicit geometric supervision. On the other hand, in the reinforced training stage, learning can be driven *solely by the outcome-based reward signal*. Specifically, as shown in Tab. 6 of the main text, even in the absence of r_{3D} there is

still an **8.93%** (68.3 vs. 62.7) improvement, indicating that *3DThinker remains robust without the teacher model.*

12. Cost

Our cost reduction primarily stems from two factors: (1) *3DThinker* typically reaches near-optimal performance within 500 training steps (see Fig. 7); (2) with VLLM acceleration, RL rollout efficiency is substantially improved. Consequently, taking Qwen2.5-VL-3B as an example, on a single H200 GPU with a batch size of 1, the convergence time for supervised training and reinforcement training is **21.84 h** and **12.85 h**, respectively.

13. More Visualization

13.1. Thinking with 3D Visualization

In Fig. 10, Fig. 11, Fig. 12, Fig. 13, Fig. 14, Fig. 15, and Fig. 16, we provide additional visualizations on MindCube-Tiny of *3DThinker-S1+S2*_{Qwen2.5-3B}, including the reasoning output, 3D imagery, etc.. *The 3D imagery (reconstructed 3D point cloud) shows what the VLM is “thinking” during spatial reasoning.*

13.2. Failure Case and Limitation

As shown in Fig. 17, we present a representative failure case. Given two images from the indoor scene, *3DThinker* incorrectly infers the spatial position of the rear object. Fortunately, by visualizing the 3D mental representation, we can identify the underlying cause. The reconstructed 3D point cloud exhibits structural inconsistencies—specifically, *the wall with two photographs is mistakenly placed on the right side of the frontal window view, whereas it should appear on the left.* This misalignment likely stems from the sparsity of the two input views, which *provide insufficient spatial constraints, leading to inaccurate 3D reconstruction and, consequently, erroneous spatial reasoning.* Therefore, in the case of extremely sparse views, better integration of other information is required, which could serve as a promising direction for future work.

Question: Based on these three images (image 1, 2, and 3) showing the same scene from different viewpoints (back, left, and right): If I am standing at the same spot and facing the same direction as shown in image 2, then I turn left and go straight, will I get closer to the wooden table? A. It would become closer to me. B. The distance wouldn't change much, but it would be on my back-right. C. The distance wouldn't change much, but it would be on my back-left. D. It would become farther from me.



3DThinker: <|latent_start|><|latent_pad|><|latent_pad|><|latent_pad|><|latent_pad|><|latent_pad|><|latent_pad|><|latent_pad|><|latent_pad|><|latent_pad|><|latent_pad|><|latent_pad|><|latent_end|>

<think> First, I have mentally constructed the 3D layout above.
 - Image 1 shows the table and chair from the back view, looking toward display cases.
 - Image 2 is the left-side view, showing the chair's back and the table edge, with more of the green-covered cabinet visible.
 - Image 3 is the right-side view, where bookshelves and cabinets are seen behind the table.
 If I'm standing at the spot and orientation of image 2 (left side), I'm facing the table and chair, with the chair directly in front of me and the table extending to my left. The green-covered cabinet is to my left, and the open space extends ahead.
 Turning left from this position means I rotate 90 degrees counterclockwise, so now I'm facing perpendicular to my previous direction—toward the open space beside the cabinets and away from the table. Going straight in this new direction means walking parallel to the long edge of the table, moving further away from it rather than approaching it.
 Thus, as I walk straight after turning left, the table—which was formerly beside me—is now getting left behind me and the distance increases. Therefore, I am moving farther away from the table.
 </think>
 <answer>D. It would become farther from me.</answer>

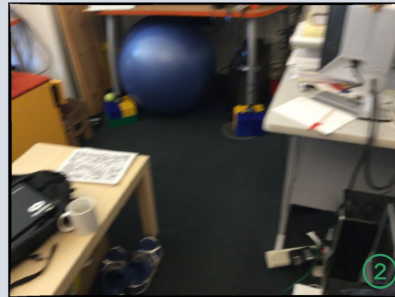
GT: D. It would become farther from me.

3D Imagining



Figure 10. More visualization results of our method. The reasoning process, GT answer, and the imagery of reconstructed point cloud from 3D latent are presented.

Question: These two images (image 1 and 2) show the same scene from two different viewpoints. Image 2 was taken after turning the camera 90 degrees to the right (clockwise) from the position of image 1. Based on these two images: If I am standing at the same spot and facing the same direction as shown in image 1, what is to my right? A. Blue ball B. Window



3DThinker: <latent_start><latent_pad><latent_pad><latent_pad><latent_pad><latent_pad><latent_pad><latent_pad><latent_pad><latent_pad><latent_pad><latent_pad><latent_pad><latent_pad><latent_pad><latent_pad><latent_end>

<think> I have constructed a 3D mental map of this room using the two images. In image 1, we see a fridge on the left side, some desks, computer monitors, and cables. There is a window in the background, centered high on the wall, providing natural light. On the right edge of image 1, the yellow cabinet and a blue ball can be seen.

In image 2, the viewpoint has rotated 90 degrees to the right (clockwise) compared to image 1. Now, most of the blue ball is visible in the center of the image, and the periphery of the room such as the table, cup, shoes, and cabinet have shifted positions relative to the ball. The right edge of this image also shows the same desk/cabinet, which links the spatial continuity to image 1.

So, if I am standing at the original spot facing the direction shown in image 1, my right side would correspond to the viewpoint seen in image 2. Since the blue ball is prominently visible in that direction after a 90-degree right turn, the correct answer for what's to my right while facing image 1's direction is A. Blue ball.

</think>

<answer>**A. Blue ball**</answer>

GT: A. Blue ball

3D Imagining



Figure 11. More visualization results of our method. The reasoning process, GT answer, and the imagery of reconstructed point cloud from 3D latent are presented.

Question: Based on these two views showing the same scene: in which direction did I move from the first view to the second view? A. Diagonally forward and left B. Directly left C. Diagonally forward and right D. Directly right



3DThinker: <latent_start><latent_pad><latent_pad><latent_pad><latent_pad><latent_pad><latent_pad><latent_pad><latent_pad><latent_end>

<think>To create the mental 3D layout, I observe that the first image shows two trash bins (Residual Waste on the left, Recyclable on the right) side-by-side, with a signboard just behind them and some trees/vegetation off to the right side and a sidewalk/hedge area to the left. The camera is facing the front of the bins directly.

In the second image, the perspective has changed: now the camera is positioned behind the bins looking toward their sides (we see the side of the Residual Waste bin and the back of the Recyclable bin). The signboard pole is now closer in view and seen from an angle, and the background details (like the road and greenery) have shifted, showing more of the adjacent pavement.

This change means the viewpoint moved from in front of the bins (Image 1) to a position further back and to the right, near the opposite corner, looking diagonally so that the bins' sides and the signboard pole are both in the foreground. The surrounding vegetation and street layout confirm this is not a simple left or right sidestep, but a movement diagonally forward and right around the bins.

Thus, the correct answer is C. Diagonally forward and right.</think>

<answer>**C. Diagonally forward and right**</answer>

GT: C. Diagonally forward and right

3D Imagining



Figure 12. More visualization results of our method. The reasoning process, GT answer, and the imagery of reconstructed point cloud from 3D latent are presented.

Question: Based on these three images (image 1, 2, and 3) showing the same scene from different viewpoints (front, left, and right): If I am standing at the same spot and facing the same direction as shown in image 3, then I turn left and go straight, what would happen to my relative position to printer? A. The distance wouldn't change much, but it would be on my front-left. B. It would become farther from me. C. The distance wouldn't change much, but it would be on my front-right. D. It would become closer to me.



3DThinker: <latent_start><latent_pad><latent_pad><latent_pad><latent_pad><latent_pad><latent_pad><latent_pad><latent_pad><latent_pad><latent_pad><latent_pad><latent_pad><latent_pad><latent_end>

<think>First, let's reconstruct the 3D layout using the three images.

Image 1 shows the front view of the printer and a small cabinet positioned side by side against a wall. Image 2 is taken from the left side of the printer, showing the left-side features, and we see the open space of the room beyond the printer. Image 3 is taken from the right side of the cabinet, looking left toward the side of the cabinet, with the open room visible beyond.

The question states that if you are standing at the same spot and facing the same direction as in image 3 (which is looking toward the side of the cabinet, with the printer and wall behind the cabinet), then you turn left and go straight.

If you are facing the direction shown in image 3, your body is oriented parallel to the wall, with the printer and cabinet on your right. Turning left means you will now face away from the wall, into the open space of the room. "Going straight" from this new orientation moves you further away from the wall (and thus from the printer, which remains near the wall).

Visualizing this: as you walk straight after turning left, you are moving perpendicularly away from the line connecting the wall and printer/cabinet. Therefore, your distance to the printer will increase.

So, the correct answer is B. It would become farther from me.</think>

<answer>**B. It would become farther from me.**</answer>

GT: B. It would become farther from me.

3D Imagining

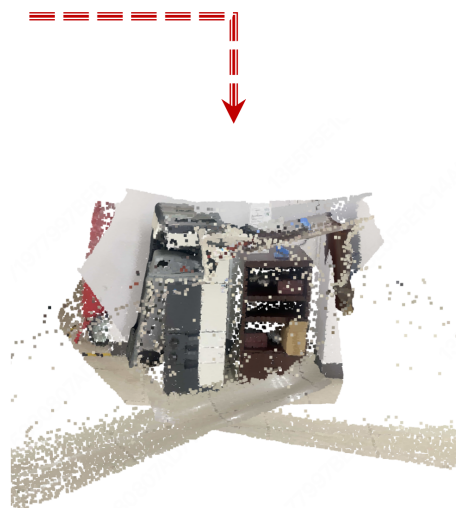


Figure 13. More visualization results of our method. The reasoning process, GT answer, and the imagery of reconstructed point cloud from 3D latent are presented.

Question: Based on these four images (image 1, 2, 3, and 4) showing the green ball from different viewpoints (front, left, back, and right), with each camera aligned with room walls and partially capturing the surroundings: If I am standing at the same spot and facing the same direction as shown in image 3, then I turn right and move forward, will I get closer to the white-red cabinet? A. No B. Yes



3DThinker: <latent_start><latent_pad><latent_pad><latent_pad><latent_pad><latent_pad><latent_pad><latent_pad><latent_pad><latent_pad><latent_pad><latent_pad><latent_pad><latent_pad><latent_pad><latent_end>

<think>

To solve this, I build a mental 3D map of the room based on the four images:

- Image 1: Facing a beige sofa with colored toys on the left. This is the "front" view.
- Image 2: Facing a brown leather couch with a red curtain behind it. This is the "left" view.
- Image 3: Facing a long white-red cabinet (white body, red top). This is the "back" view.
- Image 4: Facing a white-red counter/cabinet, a bed is next to it, and you can see further into the depth of the room, including a kitchen or dining area. This is the "right" view.

All images have the green ball and cartoon-patterned cloth in the center foreground, indicating that the table with the ball is central to all shots, and the camera positions are rotated around it.

Given the question:
 "If I am standing at the same spot and facing the same direction as shown in image 3, then I turn right and move forward, will I get closer to the white-red cabinet?"

Let's clarify directions:

- Facing "back" (image 3) means you're looking directly at the long white-red cabinet.
- Turning "right" from there means you now face in the direction that was called "right" in image 3, which is towards what appears to be the kitchen/counter area (as seen in image 4).
- Moving "forward" after turning right means walking in that direction—towards the kitchen/counter area.

The white-red cabinet shown in image 3 is also visible next to it in image 4 (to the right side). As you turn right from facing the cabinet (image 3) and move forward (towards the side shown in image 4), you actually walk alongside the white-red cabinet, getting closer to it compared to when you started (which was directly facing the cabinet).
 Therefore, moving forward after turning right does bring you nearer to the white-red cabinet/counter, matching the answer "Yes".

<think>

<answer>B. Yes</answer>

GT: B. Yes

3D Imagining

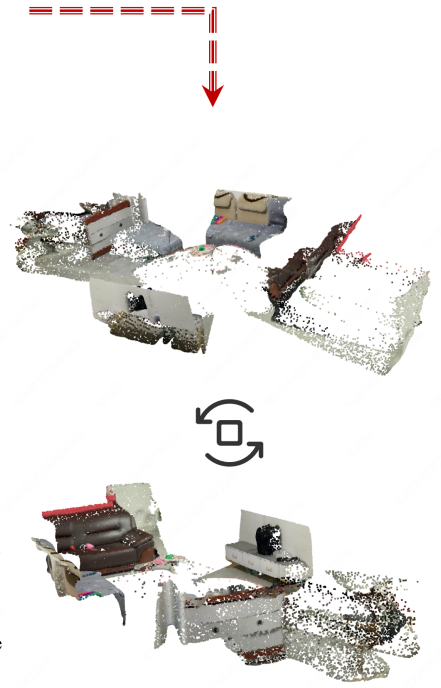


Figure 14. More visualization results of our method. The reasoning process, GT answer, and the imagery of reconstructed point cloud from 3D latent are presented.

Question: Based on these three images (image 1, 2, and 3) showing the same scene from different viewpoints (front, left, and right): From the viewpoint presented in image 3, what is the nearest object behind of the stone stool. A. planter box B. water-filled barrier C. blind passage



3DThinker:<|latent_start|><|latent_pad|><|latent_pad|><|latent_pad|><|latent_pad|><|latent_pad|><|latent_pad|><|latent_pad|><|latent_pad|><|latent_pad|><|latent_pad|><|latent_end|>

<think>

I have constructed a 3D mental model of the scene based on the three provided images. There is a paved area with red temporary barriers, a square planter box containing potted plants, and a stone stool (rectangular block).

- Image 1 (front view): Shows the face of the planter box with the stone stool to the right side, both aligned near the red barriers.
- Image 2 (left view): Provides a perspective from the left, emphasizing the planter box's oblique edge and the stone stool's position directly adjacent to the box's front face.
- Image 3 (right view): Shows the scene from the right, with the stone stool in the foreground, and the planter box extending directly behind it.

The question asks: From the viewpoint in image 3 (right view), what is the nearest object behind the stone stool?

Analyzing image 3, the stone stool is closest to the camera, with the planter box extending directly behind it in the visual frame. The red barriers and pavement tiles are further back. Importantly, the planter box is positioned immediately behind the stool, whereas the other options (blind passage or water-filled barrier) are much farther away or to the sides.

Therefore, by mentally placing myself at the right view depicted in image 3, looking at the stone stool, and considering what is directly behind it relative to my perspective, I can confirm that the nearest object behind the stone stool is the planter box.

</think>

<answer>**A. planter box**</answer>

GT: A. planter box



Figure 15. More visualization results of our method. The reasoning process, GT answer, and the imagery of reconstructed point cloud from 3D latent are presented.

Question: Based on these three images (image 1, 2, and 3) showing the same scene from different viewpoints (front, left, and right): From the viewpoint presented in image 3, is there a lamp behind the laptop? image_3.png A. No. B. Yes



3DThinker:<|latent_start|><|latent_pad|><|latent_pad|><|latent_pad|><|latent_pad|><|latent_pad|><|latent_pad|><|latent_pad|><|latent_pad|><|latent_pad|><|latent_pad|><|latent_end|>

<think>

I have mentally constructed the 3D layout based on the three images provided:

- Image 1 (front view): Shows a table with two wooden lamps on it. The laptop is placed between the lamps, and the setup is in a library environment with more tables and shelves visible in the background.
- Image 2 (left view): Gives a perspective from the left side of the table, revealing the placement of the first lamp closer to the camera. Behind this lamp, the second lamp is slightly further away, and the laptop is visible.
- Image 3 (right view): Focuses on the right side of the setup, with the right lamp prominently in the foreground. Looking past it, you see the laptop centrally positioned, and the left lamp is visible behind the laptop.

From the spatial arrangement in image 3, when standing on the right side of the table and looking straight across the setup, you observe that the lamp is placed directly in front of the laptop, only slightly separated by the table's edge. The left lamp, which is farther from the right side, is clearly visible behind the laptop from this perspective. This means that, from the viewpoint in image 3, there is indeed a lamp located behind the laptop.

Thus, the correct answer is: B. Yes

</think>

<answer>**B. Yes**</answer>

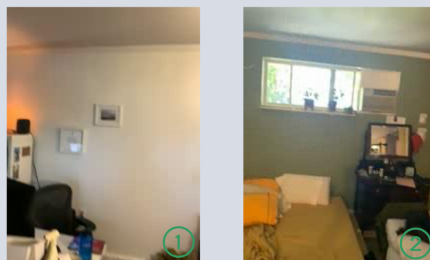
GT: B. Yes

3D Imagining



Figure 16. More visualization results of our method. The reasoning process, GT answer, and the imagery of reconstructed point cloud from 3D latent are presented.

Question: These two images (image 1 and 2) show the same scene from two different viewpoints. Image 2 was taken after turning the camera 90 degrees to the right (clockwise) from the position of image 1. Based on these two images: If I am standing at the same spot and facing the same direction as shown in image 2, then turn 90 degrees to the right, what is to my behind? A. Two photographs B. Window



3DThinker: <latent_start><latent_pad><latent_pad><latent_pad><latent_pad><latent_pad><latent_pad><latent_pad><latent_pad><latent_pad><latent_pad><latent_pad><latent_end>

<think>I have constructed a 3D scene of a room based on the two images. In image 1, I see a wall with two photographs hanging above a chair and some other furniture, including a fridge or cupboard on the left. In image 2, after rotating the viewpoint 90 degrees to the right (clockwise), I now see a window above a desk, an air conditioner, and some curtains. There is also a bed or couch beneath the window.

Given the question, if I start by facing the direction shown in image 2 (towards the window) and then turn 90 degrees to the right, my new view will be directed towards a wall not pictured here (as the wall with photographs from image 1 would be to my right after the turn). The crucial part of the question is: after making this turn, what is now directly behind me?

If facing the window (image 2) and turning 90 degrees to the right, my back will be towards the window (since it was originally in front of me before turning). Thus, the object directly behind me will be the window, matching option B.

The two photographs (option A) would be to my right or left after the turn, not directly behind. So, the correct answer is B. Window.</think>

<answer> **B. Window.**</answer>

GT: A. Two photographs

3D Imagining



Figure 17. Visualization of the failure case. The reasoning process, GT answer, and the imagery of reconstructed point cloud from 3D latent are presented.